FATIGUE SOFTENING OF COPPER SINGLE CRYSTALS

FATIGUE SOFTENING OF COPPER SINGLE CRYSTALS

by

D. H. Huggard, B. Sc.

A Thesis

Submitted to the Faculty of Graduate Studies

in Partial Fulfilment of the Requirements

for the Degree

Master of Science

McMaster University

May 1970

MASTER OF SCIENCE (1970)
(Metallurgy and Materials Science)

McMASTER UNIVERSITY
Hamilton, Ontario

TITLE : Fatigue Softening of Copper Single Crystals

AUTHOR : David H. Huggard, B. Sc. (Dalhousie University)

SUPERVISOR : Professor J. D. Embury

NUMBER OF PAGES : (v); 93

SCOPE AND CONTENTS :

The fatigue softening behaviour of copper single crystals was investigated as a function of temperature. Copper crystals, prestrained in tension, were softened by "push-pull" cycling at constant plastic strain amplitude, in the low amplitude range, and the cyclic stress-strain curves determined at various temperatures. Transmission electron microscopy was employed to determine the detailed microstructural changes which occured during softening while X-ray and slip line observations were utilized to indicate the overall structural changes on a macroscopic scale. The results were correlated and a rationale, based on dipole production, proposed for the observed softening bahaviour.

ACKNOWLEDGEMENTS

The author is deeply indebted to his supervisor, Dr. J. D. Embury, for suggesting the research problem and for continued guidance and advice throughout the course of the program.

The author wishes to thank the students and staff of the Department of Metallurgy and Materials Science for their advice, criticisms and general willingness to lend assistance in so many small ways. Special thanks are due to fellow members of the research group and to Mr. Rick Jarachowicz, for his help with the electron microscope and in various other ways.

Financial support, in the form of scholarships, from the National Research Council of Canada is gratefully acknowledged.

TABLE OF CONTENTS

		Page
CHAPTER I	INTRODUCTION	1
CHAPTER 2	LITERATURE REVIEW	5
2.1	Introduction	5
2.2	Work Hardening in Unidirectional Tension	5
2.3	Dislocation Distribution During Work Hardening	6
2.4	Work Hardening Theories	9
2.5	Seeger's Long Range Stress Theory	10
2.6	Hirsch's Stress Relief Model	11
2.7	Fatigue Hardening	12
2.8	Fatigue Softening	17
2.9	Broom & Ham	18
2.10	Snowden	19
2.11	Feltner and Laird	20
CHAPTER 3	EXPERIMENTAL PROCEDURE	23
3.1	Introduction	23
3.2	Growth of Copper Single Crystals	23
3.3	Preparation of Specimens	24
3.4	Fatigue Adaptor	26
3.5	Fatigue Cycling	26
3.6	Low Temperature Cycling	28
3.7	Slip Line Observations	29

		Page
3.8	X-ray Studies	30
3.9	Electron Microscopy	31
3.10	Outline of the Experiment	33
CHAPTER 4	EXPERIMENTAL RESULTS I - MACROSCOPIC OBSERVATIONS	34
4.1	Introduction	34
4.2	Uniaxial and Cyclic Stress-Strain Response	36
4.3	Temperature Dependence of Softening Rate	43
4.4	X-ray Results	43
4.5	Slip Line Results	45
CHAPTER 5	EXPERIMENTAL RESULTS II - ELECTRON MICROSCOPY	47
5.1	Introduction	47
5.2	Dislocation Structure During Uniaxial Tension	48
5.3	Dislocation Structure After Fatigue Softening	57
5.4	Dislocation Structure After Fatigue Softening at 195 °K	68
CHAPTER 6	DISCUSSION	70
6.1	Discussion of Macroscopic Results	70
6.2	Discussion of Electron Microscopy Results	74
6.3	Correlation of Results	78
6.4	The Saturated State	79
6.5	Experimental Errors	83
6.6	Summary	85
CHAPTER 7	CONCLUSIONS	87
CHAPTER 8	PROPOSALS FOR FUTURE WORK	89
BIBLIOGRAPHY		91

CHAPTER I

INTRODUCTION

Fatigue is a mode of deformation in which a material is subjected to cyclic stresses or strains. Most work has been done on the fracture aspect of fatigue, i.e. on the initiation and propogation of cracks leading to fatigue failure, and in predicting fatigue life, i.e. in determining the S-N curves, or plots of fatigue stress versus life to failure, for various materials. One basic aspect of fatigue of great concern is microstructural instability which arises during cycling such as the development of precipitation - free zones (PFZ) in precipitation - hardened alloys, the development of persistent slip bands (PSB), or isolated regions of localized slip from which cracks initiate and grow, and fatigue softening. (for review of the mechanisms of fatigue, see Ham (1966)).

When a pure metal is fatigued it may harden or soften depending on its initial structure (Feltner and Laird (1967)). Thus, metals in the annealed state usually harden while those that are cold worked usually soften. These changes in deformation resistance can be detected by corresponding changes in indentation hardness, flow stress, damping response and the cyclic stress-strain response of the material. During cycling these mechanical properties change rapidly at first, then slow down and approach a quasi-steady state called the saturation state. In a fatigue test in which the plastic strain amplitude is held constant, fatigue softening (hardening) is characterized by a decrease (increase) in peak stress, to a saturation value, necessary to enforce the strain limits on

successive cycles (see Figure 1.1).

Recent interest has centered on the structural changes which occur during fatigue hardening and softening and which lead to the establishment of the saturated state. An understanding of the detailed structure unique to fatigue and of the detailed mechanisms by which hardening and softening occur is important to the development of a more fundamental understanding of practical engineering problems in cyclic straining. This is true of fatigue softening in particular in relation to attempts to improve cyclic properties of metals by initial cold working.

The objective of the present study was to investigate the fatigue softening behaviour in the simple case of copper single crystals prestrained in uniaxial tension. The structure developed during tensile deformation is well understood and thus provides a good basis for studying subsequent structural changes during softening.

The experiment was designed to derive a maximum of information from a simple system. The specimens were prestrained in tension to a nominal shear stress of 4.0 kg/mm^2 and softened by cycling at a constant plastic strain amplitude of $\pm$ .0025. The cyclic stress-strain curves, or plots of peak stress on a tensile half cycle versus the number of cycles, were determined over a range of temperature and extensive electron microscopical investigations were carried out to determine the structural changes between the work hardened and fatigue softened states. Slip line and X-ray observations were used to elucidate the overall macroscopic structural changes occuring in the material during softening.

The choice of material and the strain amplitude allowed considerable scope for comparison with previous work on fatigue hardening and

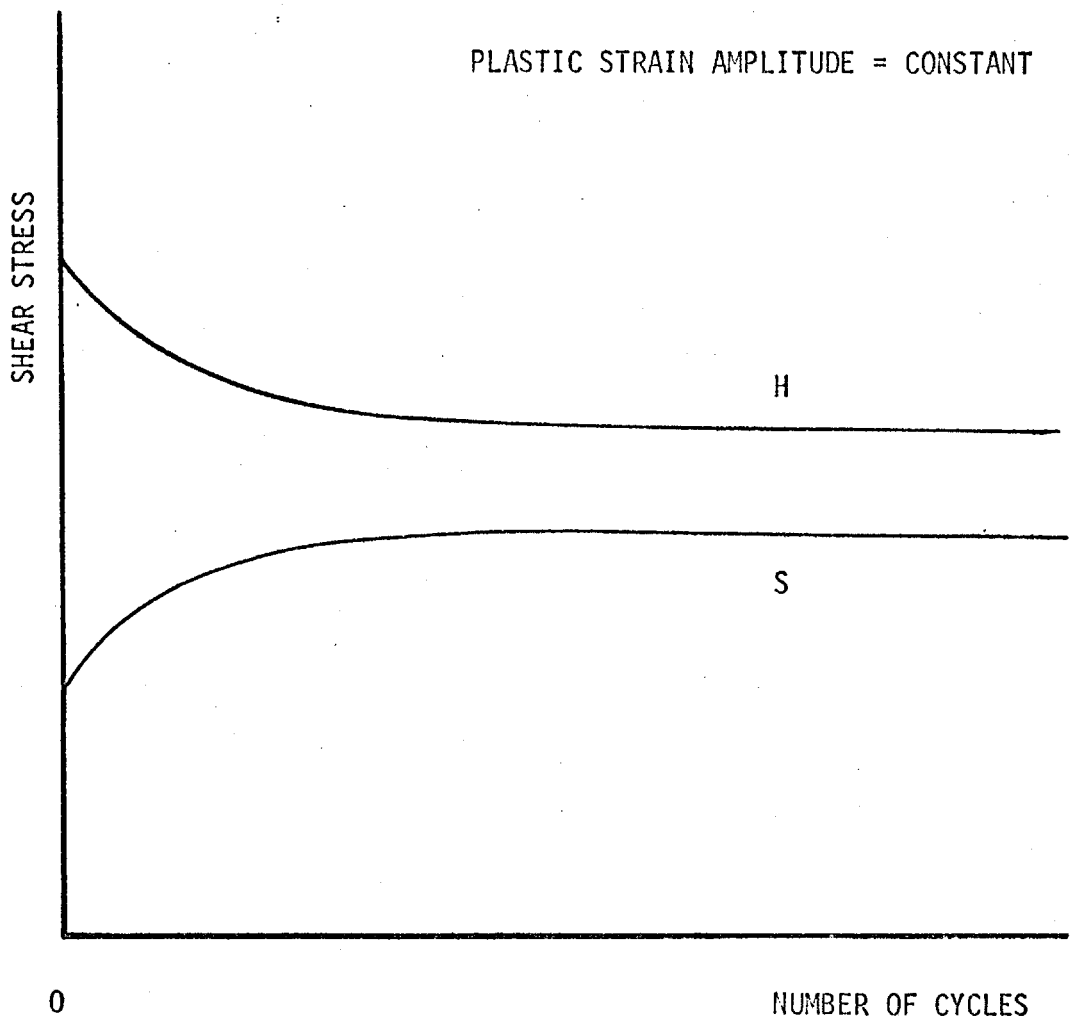

FIGURE 1.1 - THE APPROACH TO SATURATION (ZERO SLOPE) FOR AN INITIALLY HARD MATERIAL (CURVE H) AND AN INITIALLY SOFT MATERIAL (CURVE S), FOR A GIVEN PLASTIC STRAIN AMPLITUDE. FOR SOME MATERIALS, THE SATURATION HORIZONTALS FOR INITIALLY HARD AND SOFT MATERIALS MAY COINCIDE.

unidirectional hardening while the behaviour at various temperatures allowed conclusions to be drawn concerning the extent to which softening is controlled by thermally activated processes. The development of a dislocation model to account for the observed facts is important to a fundamental understanding of fatigue softening and indeed of the cyclic behaviour of metals in general.

CHAPTER 2

LITERATURE REVIEW

2.1 Introduction

The present investigation is concerned with the mechanical behaviour of copper single crystals subjected to cyclic straining after a prestrain in uniaxial tension. Thus it is pertinent to review briefly the hardening mechanisms occuring during work hardening in uniaxial tension with emphasis on the nature of the microstructure which is developed. In addition, certain dislocation mechanisms are unique to the cyclic mode of deformation and are understood mainly in connection with work done on fatigue hardening. Therefore, the relevant aspects of the literature on both work hardening and fatigue hardening will be included in the present review as well as work concerned specifically with fatigue softening.

In discussing both results reported in the literature and in the present investigation, the Steeds system of notation (Steeds (1966)) for the slip systems will be used. (see Figure 4.1)

2.2 Work Hardening in Unidirectional Tension

Many of the fundamental investigations of work hardening in f.c.c. metals have been concerned with explaining the general shape of the stress-strain curve of single crystals. In general these exhibit three stages. Stage I, or easy glide, is a region of low hardening, of order $\mu/2000$, which is present to any appreciable extent only in crystals oriented for

single slip. In stage II the stress varies linearly with strain and the region, with hardening rate of order $\mu/200$, is known as "linear hardening". Most of the structural investigations have been concerned with this region. Stage III shows a gradual decrease in hardening rate and is often called the parabolic hardening region although in general, no parabolic relation between stress and strain exists.

A great deal of work has been done in an attempt to determine the mechanisms of dislocation interaction to explain hardening and the process of dislocation accumulation in stage II. Current theories attribute hardening to a variety of mechanisms, including long range stresses from piled up groups of primary dislocations, stresses induced by the dragging of jogs on screw dislocations, stresses necessary to bow out segments of dislocation networks, and interactions with forest dislocations.

Comprehensive reviews correlating present theories of work hardening and summarizing experimental results have been published by Nabarro, Basinski and Holt (1964), by Clarebrough and Hargreaves (1959) and by the Metallurgical Society Conference on Work Hardening (1966).

Of particular relevance to the present work is the detailed form of the dislocation structures developed during work hardening as revealed by X-ray methods and electron microscopy. A number of studies have been published in the past seven years, notably: Steeds (1966), Basinski (1964), Steeds and Hazzledine (1964), Hirsch (1963) and Mader, Seeger and Leitz (1963). A summary of their results is the basis for the following section.

2.3 Dislocation Distribution During Work Hardening

The salient features of the microstructure in deformed copper

crystals were similar in all investigations and were generally described with respect to the particular region of the stress-strain curve to which the crystal had been deformed.

Stage I: The predominant feature of the dislocation structure consists of bundles of primary edge dislocations lying along $[1\bar{2}1]$. The bundles themselves are often elongated along this same direction or along the intersection of the primary plane with the conjugate and critical planes. The bundles occupy only a small fraction of the area of the foils and have in general some forest dislocations associated with them. At the end of stage I the secondary dislocation density comprises 5 to 20% of the total. The lack of lattice rotations, revealed by both electron microscopy and lack of X-ray asterism, indicate that the bundles consist of approximately equal numbers of positive and negative dislocations and most appear to be associated as dipoles. It is significant that, while dipoles are a prominent feature of stage I, they become less important in stage II or even in the earlier stages of crystals oriented for multiple slip.

Stage I - Stage II: The transition into stage II is accompanied by an increase in activity of the secondary systems and many more dislocations, particularly of the critical and conjugate systems, are observed. These secondary dislocations are associated with the dipole tangles and there is evidence for interaction between primary and secondary dislocations. The resulting reacted dislocations have short meshlengths indicating that secondary slip is local.

Stage II: At the beginning of stage II there is a considerable

accumulation of barriers, consisting of the forest dislocation - primary dipole tangles which are aligned in the primary plane along the traces of the conjugate and critical planes. With increasing deformation many more tangles form, their alignment becomes more irregular and there is an increasing tendency for dense patches of dislocations to cluster together in directions out of the slip plane. At the end of stage II the tangles form a ragged cell structure when viewed in sections parallel to the primary plane and some of the dense bands of dislocations show misorientations of approximately 1° across them. The networks, again viewed in sections parallel to the primary plane, consist largely of primary dislocations and Lomer-Cottrell dislocations formed by the reaction of primary dislocations with those of the conjugate or critical systems. A second type of region has been observed in copper, particularly in crystals deformed at 4.2 °K, which persists throughout stage II. These are "bundle regions" which consist of primary edge bundles, similar to those of stage I, but much denser and more irregular. They rarely show evidence of lattice rotation and are composed of short dipole segments resembling those observed in fatigued copper crystals. One striking feature, observed in all sections, is the relative absence of screw dislocations, so that screws do not appear to accumulate, at least in copper, during deformation.

Stage III: The networks become more dense and the lattice tilts produced across them become much more pronounced. The configuration can be described as dislocation sheets lying approximately parallel to the primary plane, their separation gradually decreasing with increasing deformation. It should be emphasized that the dislocation structure is still

highly non-uniform with the bundles and networks separating regions of the crystal still relatively dislocation free. In regard to the lattice rotations observed, there is no general agreement concerning their nature. Various investigators have observed different axes of rotation and have identified the networks as tilt boundaries and as twist boundaries. It is still not clear whether the discrepancies are due to different testing variables or to fluctuations in the sampling of the boundaries observed.

In stages II and III the density of secondary dislocations becomes comparable to that of primary dislocations. Dislocation counts by Steeds and Hazzeldine (1964) put the density of secondary dislocations as high as 60% of the total density for stage II.

2.4 Work Hardening Theories

As previously mentioned, a great many work hardening theories have been presented, most of which deal with the linear hardening part of the stress-strain curve and all of which result in the relation that the flow stress is proportional to the square root of dislocation density. Basinski (1965) broadly classifies the theories into two groups: those ascribing the flow stress to interactions between the primary dislocations, singly or in groups, and those concerned with the interaction between the primary dislocations and the dislocation forest.

As examples of the two types of models, Seeger's long range stress theory (Seeger (1963)) and Hirsch's stress relief model (Hirsch (1964)) will be considered. The choice of these two models is particularly significant to the present work since they reveal a basic difference in reliance on, and confidence in, electron microscopical observations.

2.5 Seeger's Long Range Stress Theory (Seeger 1963)

The transition from stage I to stage II is related to the onset of secondary glide but the enhancement of the work hardening rate is not due to a direct interaction between the primary and forest dislocations. Rather, the primary and forest dislocations interact to produce obstacles against which the primary dislocations pile up. He suggests obstacles such as sessile dislocations (e.g. Lomer-Cottrell locks). The flow stress is then calculated as the maximum stress necessary to move a dislocation through the softest part of the crystal, that is half-way between piled-up groups of dislocations (which he approximates as giant dislocations of Burgers vector nb).

Seeger's theory is in excellent agreement with slip line observations and macroscopic measurements and with electron microscopical results to the extent that he considers them valid. He emphasizes the obvious point that a thin foil cannot be completely representative of the bulk sample and refers to considerable evidence of dislocation loss and rearrangement during foil preparation. He also makes the point, often overlooked, that in interpreting electron micrographs the tendency definitely exists to overrate those features which can be seen clearly. As an example he cites the fact that electron microscopy is in general unsuitable for revealing directly the presence of long range stresses. In this regard, however, Mughrabi (1968) has recently succeeded in observing pile-ups of from 10 to 20 dislocations in deformed copper crystals by neutron irradiating the specimens before unloading (neutron irradiation "pins" the dislocation structure). He also observed screw dislocations in much greater numbers than previously reported and concluded that

fairly extensive rearrangement of dislocations must have occurred during unloading.

2.6 Hirsch's Stress Relief Model (Hirsch 1964)

Stage I produces some kind of barriers to slip and internal stresses of piled-up groups of primary dislocations are relieved by secondary slip. At the beginning of stage II piled-up groups are so close that secondary sources operate everywhere in the crystal.

At this stage, the structure consists of long continuous obstacles which block the slip lines all way round. As the stress is increased, a new slip line is formed and the dislocations propogate until they approach existing obstacles long enough to block the slip line all way round. The dislocations thus pile up causing the total shear stress to increase sufficiently to activate the nearby secondary sources and the newly formed slip line becomes a complex obstacle itself. Each slip line acts as an obstacle to further slip so that regions of high dislocation density trap more dislocations, resulting in a non-uniform distribution and the development of a cell structure. Since the dislocations on the secondary systems move only small distances, of the order of pile-up spacings, the strain carried by the secondary systems is small although the dislocation density may be high.

As formulated, the theory explains satisfactorily a number of experimental facts such as hardening rate, slip line length, number of dislocations per slip line, the large secondary dislocation density but small plastic strain on secondary systems and the formation of a non-uniform structure. Perhaps its most significant shortcoming is that it fails

to predict the relative contributions of forest dislocations, internal stress, jogs, etc. to the flow stress.

Hirsch (1963) seems more confident in accepting the validity of electron microscope results than does Seeger. He discusses in detail the problems of dislocation loss and rearrangement during thinning and compares electron microscope results to those by other methods such as X-ray and etch pitting techniques. He concludes that, at least for copper deformed such that the scale of the substructure is small compared to foil dimensions, the observed substructure is truly representative of the bulk sample. Under these conditions, dislocation loss and rearrangement should be very small. This is supported by an experiment reported by Basinski (1965) in which the dislocation structure in deformed copper was pinned by neutron irradiation before thinning and found to be quite similar to the structure in unirradiated samples.

Hirsch also discusses the problem of underestimating dislocation densities because of image overlap and invisibility due to contrast effects and points out that these errors are correctable by considering micrographs taken in various reflections and of various sections of the crystal. He recognizes, however, that there is a problem and stresses the need for more detailed knowledge of the mechanisms and degree of rearrangement.

2.7 Fatigue Hardening

Compared to the many detailed models based on fairly consistent experimental results found in work hardening, the situation concerning fatigue hardening is somewhat different. While there exists a great deal

of experimental evidence, the variety of testing modes used, i.e. constant stress amplitude, constant strain amplitude, push-pull cycling, torsion cycling, etc., makes direct comparison difficult. The situation is further complicated by the difference in cyclic behaviour exhibited by metals subjected to low amplitude and to high amplitude (relative terms which vary from one investigator to another) fatigue.

Much of the early work on fatigue concerned the saturated state and not the hardening state. (In cycling at constant plastic strain, the initial cycles show a rapidly increasing peak stress while the later cycles show very little increase in peak stress; this latter period is known as the saturated state). Very recently, several investigators have followed in detail the development of the dislocation structure during the hardening stage, from the early cycles up into saturation. The work on copper single crystals cycled in "push-pull" has the greatest relevance to the present research and will be reviewed here.

Shinozaki and Embury (1969) cycled copper single crystals at low amplitudes and examined sections parallel to and perpendicular to the primary slip plane by transmission electron microscopy. They established that numerous dipoles are formed early in hardening which are initially randomly distributed and sometimes arranged in complex configurations. At later stages, extensive arrays of dipoles are formed by interaction between parallel groups of dislocations and complex braids of dislocation debris are formed containing large numbers of dipoles and primary edge monopoles aligned along $[\bar{1}01]$, $[1\bar{1}0]$ and $[\bar{1}2\bar{1}]$ of the primary slip plane. These braids contain extensive walls of dipoles perpendicular to the primary planes and mats of dipoles parallel to the primary planes.

As cycling continues, the braids become more clearly defined and their spacing decreases rapidly to a constant value of 1.5 μ, reached at about 200 cycles. The detailed structure of the braids is complex, containing a variety of hardening obstacles such as Lomer-Cottrell locks and faulted dipoles and resembles that reported for stage I - early stage II unidirectional deformation. One important difference is the lower density of secondary dislocations produced in the cyclic case.

Hardening is attributed to the interaction of parallel dislocations of the primary or coplanar systems moving on the primary plane and the creation of a large number of dipoles. The dipoles appear to form by both jog dragging and termination mechanisms (Johnston and Gilman (1960)) and by the interaction of parallel dislocations of opposite signs. They initially accumulate in the vicinity of forest dislocations, where the shear stress on the cross-slip system is amplified sufficiently to allow cross slip (Bullough and Sharp (1965)).

At saturation the imposed strain must be carried by the motion of dislocations between the braids or by localized rearrangement within the braids. Slip line evidence indicates that surface slip activity continues during saturation so that at least a portion of the strain is borne by dislocation motion between the obstacles.

Hancock and Grosskreutz (1969) cycled copper single crystals in push-pull at a constant total shear strain amplitude of $\pm$ .0075, which is considered to be in the intermediate to high amplitude range. From their electron microscopy on foils parallel to and perpendicular to the primary slip plane, they observed a dislocation structure similar to that reported by Shinozaki and Embury during the initial rapid hardening stage,

and the development of a two dimensional cell structure when saturation is approached. In particular, the principal dislocation interaction during rapid hardening is the mutual trapping of primary dislocations on parallel slip planes which result in bundles of dipoles and multipoles aligned along $[1\bar{2}1]$, $[1\bar{1}0]$ and $[0\bar{1}1]$ and which thereby develop as obstacles to further dislocation motion. By 20 cycles the bundles have become more dense, the density of secondary dislocations is approximately equal to that of the primaries, the bundle density has increased and the dipoles within the bundles are fragmented into much shorter lengths. As saturation hardness is approached, the development of the cell structure is nearly complete and the secondary dislocation density now equals or exceeds the primary dislocation density. As hardening progresses, the bundles are continuously fragmented into dense tangles of short dislocation segments, loops and dipoles which are unique to cyclic deformation. The remaining few per cent of hardening is a result of extending the dislocation network in a direction normal to the primary slip plane.

The problem of strain accomodation at saturation was considered and calculations showed that in the case of intermediate to high amplitude fatigue, either dislocation motion across cells or co-operative movement of dislocations within cell walls would account for only about one-half the energy dissipated in the specimen each cycle. The remaining energy was then available for point defect production and as heat loss.

The authors also concluded that there was no basic difference between low and high amplitude fatigue behaviour. Rather, they concluded, the mechanism of production of loop patches in low amplitude cycling and of cell walls in high amplitude cycling are identical. The effect of the

high amplitude was to promote the organization of the patches (formed at all amplitudes) into a regular cell structure.

Similar dislocation structures were reported by Basinski, Basinski and Howie (1969) who cycled copper single crystals at a plastic strain amplitude of 3.25×10^{-3}. They found an excellent correlation between the dislocation distributions obtained by etch pitting and by electron microscopy for both the primary and the cross-glide plane and observed that three stages could be recognized in the build-up of the microstructure. In the first few cycles the dislocation structure is similar to that of stage I of tensile deformation, with dislocations lying approximately parallel to the glide plane. Later, walls of dislocations form in the kink band direction on the cross-glide plane and a cell-like structure with two kinds of region builds up on the primary plane. The scale of the structure decreases with increasing number of cycles. The third stage is characterized by a spotty dislocation structure on the cross-glide plane caused by a break-up of the walls.

In most of their photographs a large number of unresolved small black spots were observed, more clearly during later stages of fatigue. Since no mottling of this kind was observed in pure tension, they speculated that it represents the agglomeration of point defects produced in large numbers during fatigue.

Intense slip lines were not normally observed, but this was only true if the plastic strain limits were accurately controlled and not exceeded. Even a small overshoot by a strain of $2\text{-}3 \times 10^{-4}$ resulted in the formation of strong prominent slip lines. These behaved very similarily to the intense slip lines showing a high degree of reversibi-

lity which were observed by Watt et al (1968) at very much higher cumulative strain. This effect indicates that a crystal is "trained" to a particular fatigue cycle and that the mode of deformation changes drastically when this is exceeded.

The merits of various proposed mechanisms for fatigue were discussed and the conclusion reached that many of the properties of deformation by fatigue and differences from deformation in tension can be rationalized if the flow stress during fatigue is attributed to the presence of point defects in the lattice.

2.8 Fatigue Softening

When subjected to fatigue, an annealed pure metal will usually harden while a cold worked metal will in general soften. Although a relatively large amount of work has been done on fatigue hardening, very little has been published on the opposite phenomenon and many of the known facts in regard to fatigue softening have arisen coincidentally in the course of other investigations,

For the purpose of this review, three papers in which fatigue softening was investigated to a major extent and in a manner pertinent to the present research will be discussed. Broom and Ham (1962) studied the mechanism of fatigue softening in copper single crystals, Snowden (1963) included softening characteristics in his study of the cyclic behaviour of aluminum single crystals and Feltner and Laird (1967) published a comprehensive paper on cyclic hardening and softening of polycrystals of copper and copper -7.5% aluminum.

2.9 Broom and Ham (1962)

Broom and Ham prestrained copper single crystals in tension and softened them using "push-pull" fatigue stressing at various temperatures between 78°K and 293°K. For a given prestrain and temperature, they determined the minimum fatigue stress which would cause softening in 10^5 cycles and checked that such softening had actually occured by observing a decrease in yield stress of the sample in a subsequent tensile test.

They postulated three phenomena on which the mechanism of softening could possibly be based: (a) Bauschinger effect - for a specimen prestrained in tension, the compressive yield stress is low so that during the compressive half cycles of stress, unlocking of dislocations are possible. (b) Climb by point defects - point defects generated by fatigue can cause climb of locked dislocations and so initiate new sources, to give a more uniform dislocation distribution. (c) Striation formation-slip striations form in metals fatigue softened at room temperature and are believed to be soft regions of the softened metals. By relating the stress at which slip bands coarsen in tensile specimens with the stress necessary for striation formation in fatigue, and assuming cross-slip or barrier breakdown to be the fundamental dislocation process, a correlation between cross-slip and striation formation is possible.

Their experimental results showed that the minimum stress necessary to cause softening in 10^5 cycles, τ_{fs}, increased slightly with increasing prestrain and decreased markedly with increasing temperature. They plotted τ_{fs} along with τ_{III}, the stress corresponding to the end of stage II hardening and to the onset of profuse cross-slip, and a parameter τ known to show the same temperature dependence as the Bauschinger effect as a function of

temperature. The softening stress τ_{fs} varied with temperature in a manner closely similar to τ_{111}, both much more strongly than τ.

Metallographic examination showed that the onset of softening was associated with the appearance of short wide slip markings, that the first visible slip lines when a softened specimen was slighly extended coincided with the striations produced by softening, and that a high density of striations were produced when the softening stress was well above the necessary minimum.

Broom and Ham conclude that cross-slip is the fundamental process of striation formation and that striation formation is essential for fatigue softening. Concerning the role of the Bauschinger effect and of point defects, they draw no definite conclusion but feel they may play a contributory part in the softening process.

2.10 Snowden (1963)

Snowden did some softening experiments on aluminum single crystals in conjunction with cyclic hardening tests. The crystals were initially hardened by high amplitude fatigue (100 cycles at $\gamma_p = \pm .005$) and then softened by smaller cyclic strains ($\gamma_p = \pm .0007$) and the resulting stress-strain loops plotted for the first twelve softening cycles. This showed that part of the initial rapid softening was simply a geometrical effect due to the shape of the loops and that a more gradual "secondary" softening occured which restored the original symmetry of the loops.

He interpreted the cyclic softening process in terms of the accomodation of the smaller imposed deformation by the reversible movement of the abnormally high number of dislocations introduced by the original large

strain amplitude. The reversible movement of dislocations allows for further dislocation interactions, annihilations and the adoption of positions of lower potential energy. Electron microscopy observations suggested a somewhat lower dislocation density in the softened state but no quantitative analyses of the structures were performed.

2.11 Feltner and Laird (1967)

Feltner and Laird studied cyclic hardening and softening in polycrystals of Cu and Cu-7.5% Al and examined the effect of (a) slip mode of the material, (b) its initial condition as governed by cold working and annealing treatment, (c) temperature and, (d) cyclic strain amplitude.

In general, they determined that all f.c.c. metals harden or soften under cyclic straining to a characteristic saturation or steady state flow stress which is attained at most after 50% of fatigue life. In particular, for wavy slip mode materials there exists a cyclic mechanical equation of state; that is, the saturation flow stress is a unique function of strain range, strain rate and temperature and independent of prior strain history. In the case of planar mode materials, however, they found the steady state stress to be a sensitive function of thermal and deformation history. In both materials, the transient stage of hardening or softening was not strongly affected by slip mode or temperature.

From an investigation of the cyclic softening of copper, they found that in general, the softening rate of cold worked copper usually increases as the strain amplitude decreases. However, from their own and collected data, the softening rate was seen to reach a maximum at a

strain amplitude giving a life to failure of the order of 10^4 cycles. Decreasing the strain amplitude past this value caused a decrease in softening rate which eventually approached zero at some none-zero strain range. At this point, softening fails to occur.

Feltner and Laird postulate that a prerequisite for cyclic strain softening is a reversed plastic strain. They demonstrated this by cycling a prestrained copper specimen for 10^5 cycles at various values of the compressive stress limit. They found that no softening occured when this stress limit was below a certain threshold stress which they showed to be the minimum stress at which measurable reversed plastic strain occurs.

From quite extensive observations of the dislocation structures developed in strain cycled copper, using electron microscopy, the authors found in general: (a) regardless of structure prior to cycling a cell structure is always observed after cycling at strains giving lives less than 10^4 cycles, (b) the saturation cell size is independent of the initial condition of the metal, increases as the test temperature increases, and increases as the strain amplitude decreases and (c) the cell wall structures are independent of the initial conditions of the material and are often in low energy configurations such as twist boundaries.

The qualitative picture of fatiuge softening as discussed by Feltner and Laird is that, since the saturation stress in wavy slip mode materials is a unique function of strain range, strain rate and test temperature, initially cold worked materials must go through an appreciable transient stage before reaching saturation. Thus considerable cyclic plastic strain may be required to revert the initial deformation structure to one characteristic of the cyclic condition. That such structural reversion actually

occurs is apparent on the macroscopic scale from changes in indentation hardness, flow stress, stored energy of cold work, X-ray back reflection photographs, electrical resistivity and other properties which depend on the arrangement and density of dislocations.

Under some conditions, such as when the cyclic strain amplitude is small or when cross-slip is difficult, as in planar slip mode materials, the softening process may not be complete. This is due to the fact that a basic change in type of dislocation arrangement is necessary. Thus, materials work hardened by high strain fatigue or by unidirectional deformation form a cell structure which, when cycled at low amplitude, must be reverted to a dipole structure for complete softening. On the other hand, softening by high amplitude requires only a change in the "degree" or "intensity" of the structure.

In wavy slip mode materials like copper, it is this three dimensional dislocation motion via cross-slip which allows such dislocation rearrangement. However, although cross-slip may allow complete softening, it does not control the rate of softening. Evidence suggests that the rate controlling processes are jog dragging or forest cutting processes. This is consistent with the higher softening rate in Cu-7.5% Al than in Cu which contains dislocations which are heavily jogged and tangled.

Many experiments have shown that point defects are produced in large numbers during cyclic straining. The eventual annihilations of these point defects would also tend to add completeness to the softening process in wavy slip mode materials.

CHAPTER 3

EXPERIMENTAL PROCEDURE

3.1 Introduction

The main objectives of the research were to obtain the cyclic stress-strain softening curves for copper single crystals of identical orientation at various temperatures and to determine the detailed dislocation microstructure developed. To this end, details of the procedure for the growth and preparation of specimens, fatigue cycling and preparation of thin foils for transmission electron microscopy are outlined in this chapter. An additional aspect of the experiment was the correlation of the previously mentioned results with slip line and X-ray observations, the experimental aspects of which are included.

3.2 Growth of Copper Single Crystals

Five single crystals of the same orientation were required for the experiment so that, in order to avoid use of a seed, one single crystal at least 13" long had to be produced.

The crystals were grown of OFHC copper of 99.995% nominal purity, supplied by M & T Metal Company Ltd., Hamilton, Ontario, Canada, in a long cylindrical mould of high purity graphite. The mould was 15" long, had an outside diameter of 3/4" and had a 7/16" diameter hole bored completely through its length. The bottom end of the mould was

equipped with a tightly fitting graphite plug, the top of which had a drilled hollow point, which was held in place by a small ceramic pin extending through both mould and plug. The removable end plug made possible the easy removal of the crystals from the mould.

The crystals were grown by lowering the mould slowly, at a rate of 2"/hr., through a vertical furnace maintained at a temperature of 1200°C. The mould was supported through the hot zone of the furnace by heavy gauge Kanthal wire and oxidation of the mould was prevented by passing it inside a 1-1/4" I.D. mullite tube, 4' long, in a reverse flow of nitrogen.

The resulting crystals were checked for grain boundaries in a $FeCl_3$ etch described by Barrett (1959) (1 part HCl, 1 part H_2O saturated with $FeCl_3.6H_2O$). Alternate immersion in this solution and a 40% solution of nitric acid resulted in a surface which clearly showed the crystallographic planes with different reflectivities. As an additional check, Laue back reflection X-ray patterns (see Section 3.8) were taken at either end and at various points along the length.

Several attempts were made until finally a single crystal, approximately 13" long, was obtained.

3.3 Preparation of Specimens

From the 13" crystal, five pieces each 2.5" long were carefully cut with a jeweller's saw. The original crystal had been carefully marked so that the mutual orientation of the pieces was retained. The crystals were then sealed individually in vacuum and annealed for 24

hours at 950°C followed by furnace cooling.

Gauge lengths 1" long and of square crossection were produced in the specimens by spark maching on the Servomet sparkcutter. The crystal was held in a horizontal position and a face was machined to the desired depth using as a tool a rotating cylinder of graphite 1" in diameter. The crystal was then rotated 90° about its axis and the second face was machined to the same depth as the first. Continued in this way, the procedure resulted in four flat faces machined to equal depths and defining a crossection square in shape. It should be noted that although the orientation of the parallel faces was chosen at random, consistency was maintained from one crystal to another.

The graphite tool tended to wear at its center at a faster rate than at its extremities and thus had to be remachined flat at intervals of approximately 40 minutes. For this reason a number of graphite "caps" each 1" in diameter, were machined to fit tightly over a smaller diameter brass cylinder. In this way, an unevenly worn tool could be quickly replaced and resurfaced at leisure.

The ultimate crossection desired in the gauge length was 1/4" x 1/4". Since the depth of damage due to spark planing, as reported by Shinozaki (1968), is about .3 mm (.013") a crossection of 0.29" x 0.29" was produced by spark machining. The crossection was reduced to the desired dimensions by chemical polishing in a solution of 50% nitric acid in water followed by electropolishing using D2 electrolyte (200 ml phosphoric acid, 500 ml distilled H_2O, 250 ml ethanol, 2 ml Vogel's Spaibeize[1], 50 ml propanol, 5 gm urea) at approximately 10 volts. The

[1]Trade Name

chemical polish resulted in a flat, even attack while the final electropolish produced a smooth shiny surface.

The specimens were again individually vacuum sealed and annealed for 24 hours at 950°C. Each specimen was again electropolished immediately before testing.

3.4 Fatigue Adaptor

The cyclic straining modification to the Instron TTC-L was designed and constructed by Watt (1967) and a full description of its advantages, specifications and design have been given in Watt's thesis (1967). The most important feature of the adaptor is its open cage design which allows, as well as "in situ" electropolishing and surface replication of a specimen, the complete immersion of specimen and grips in a constant temperature bath for tests at temperatures other than room temperature.

3.5 Fatigue Cycling

The initial tensile deformation of the specimens, to a nominal resolved shear stress of 4 kg/mm^2, was done using the fatigue adaptor and with the specimens mounted and aligned according to the procedure detailed by Watt (1967).

After tensile deformation the specimens were cycled at constant plastic strain amplitude of $\pm$ .0025 which was measured directly off the Instron chart recorder. The speed of the crosshead and of the chart were synchronized so that by extending the elastic curve on the chart recorder (see Figure 3.1) the plastic elongation could be measured off while the

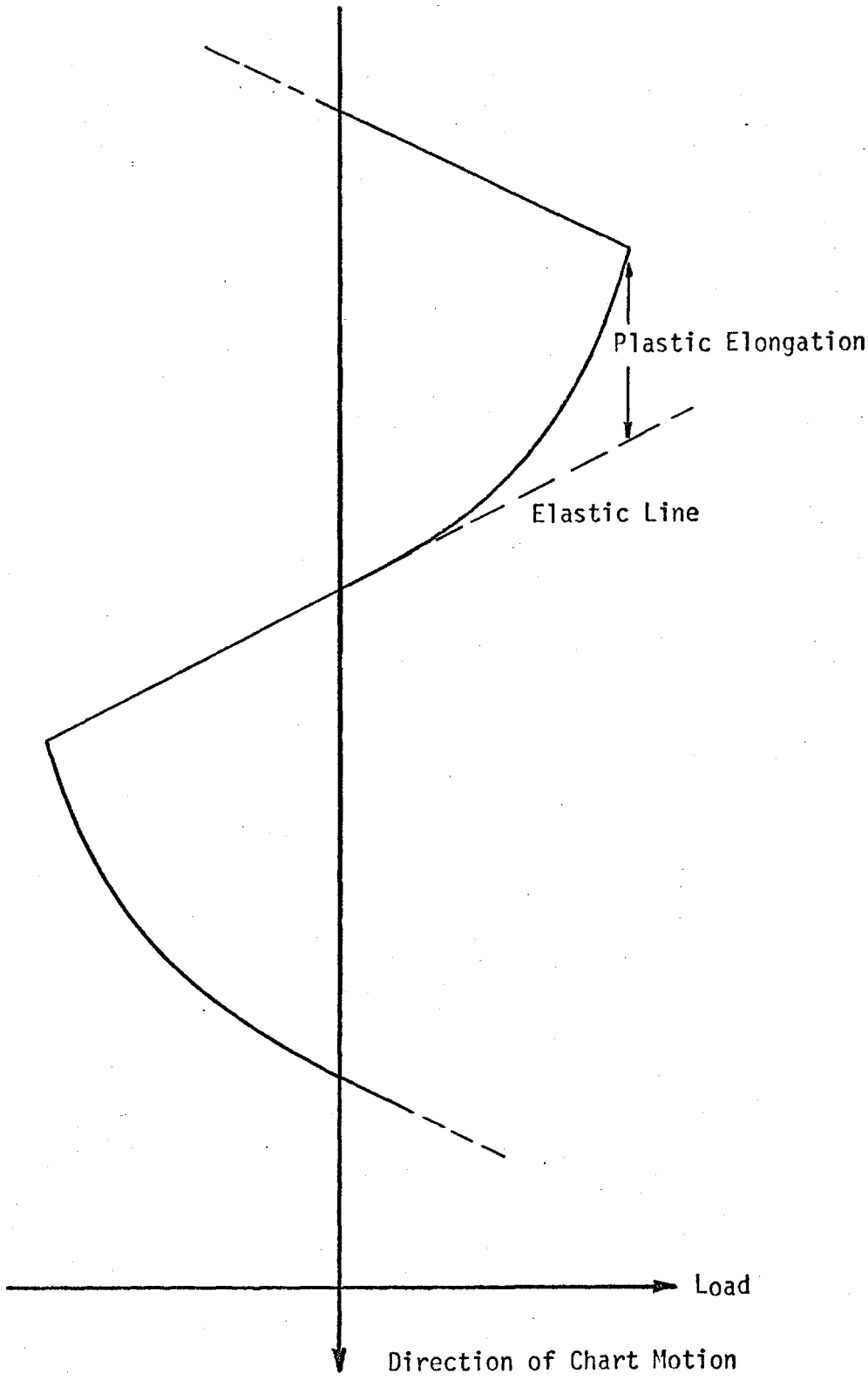

FIGURE 3.1 - DETERMINATION OF PLASTIC STRAIN DURING CYCLING

chart was moving. When the plastic elongation corresponding to the predetermined plastic strain amplitude was approached, the direction of the crosshead was manually reversed. The first 100 cycles of each specimen were done under manual control and at a crosshead speed slow enough to ensure an accuracy of at least $\pm$ 5% in the measurement of plastic strain amplitude. After 100 cycles the softening rate was low enough to permit cycling controlled by the extension limit switches. In this mode of operation, limits to the motion of the crosshead in either direction are preset and the crosshead motion is automatically reversed when these limits are reached. The load-elongation curve had then only to be checked periodically and slight adjustments made to the extension limits when necessary.

3.6 Low Temperature Cycling

Part of the experiment necessitated cycling at temperatures much lower than room temperature. This was accomplished by immersing the entire lower cage assembly, including the specimen, into a large dewar flask filled with liquid at the desired temperature.

One test was done using dry ice in ethanal, a mixture which equilibrates at -78°C. By maintaining an excess of CO_2 in the mixture and by occasional stirring, the temperature of the bath could be held constant to within 2°C of the equilibrium temperature.

A second test was run at a temperature of -26°C $\pm$ 1°C in a mixture of liquid Freon and ethanol. This mixture cools to various temperatures depending on relative proportions, the ratio used in this case being experimentally determined. The temperature of this bath could be held to

within ± 1°C by occasional addition of a small amount of Freon and by stirring.

In both cases the specimen had to be slowly cooled by gradual lifting of the bath around the cage of the adaptor. Differential coefficients of thermal expansion of the stainless steel fatigue adaptor and of the copper specimen could strain the specimen to loads of many tens of pounds so that the crosshead had to be continually adjusted during the cooling stage. The cage and specimen were allowed to equilibrate at the temperature of the bath for at least four hours, during which time the load was monitored on the chart recorder, before fatigue cycling was started.

It was found that the specimen could be left in either bath overnight (12 hrs) during which time the temperature rose about 10°C. This caused a load on the specimen of less than 10 pounds.

3.7 Slip Line Observations

Detailed slip trace analysis was not planned as part of the experiment but a knowledge of the cumulative slip line topology after the various modes of deformation was desired. For this purpose optical replicas were taken from the specimen surfaces after tensile deformation and again, the specimens having been electropolished before start of cycling, after fatigue softening at the various temperatures.

The replicating material was .005" thick cellulose acetate sheet with a matte finish on one side. A drop of acetone from a squeeze bottle was placed on the specimen face to be replicated and a thin strip (approximately 3/4" x 1/4") of the plastic was immediately placed over the acetone

drop, shiny side down, and held firmly for about a minute. Pressure was carefully released and the replica allowed to dry on the specimen for half an hour before being slowly stripped from the surface. The replicas were mounted with tape on glass microscope slides.

At least four replicas were taken from each specimen and the better quality ones were then "shadowed" with approximately 100 Å of aluminum deposited by vacuum evaporation. Evaporated onto the surface at an angle of 10°, the aluminum increased the reflectivity of the replicating surface and increased the contrast of the slip lines by depositing preferentially on one side of the lines.

The slip lines were examined in a Reichert optical microscope and photographs were taken, at a magnification of X200, using Polaroid Polopan film. Only the slip lines from the tensile specimens were photographed from replicas, the slip lines from the fatigue softened specimens being photographed directly from the specimen surfaces.

3.8 X-ray Studies

Laue back-reflection X-ray patterns were used to check the perfection and orientation of the single crystal specimens. In addition, some information concerning the nature of the dislocation substructure developed during deformation could be inferred from qualitative estimates of the degree of asterism exhibited in the Laue spots.

X-ray photographs were taken using the Philips X-ray diffraction generator, model PW 1010, with a tungsten tube and unfiltered radiation. Operating conditions were 50 kV and 12 mA, specimen to film distance was the standard 3 cm and in all cases exposure time was 15 minutes.

In order to check the degree of asterism developed during the strain history, Laue photographs were taken of the specimens in the undeformed, pulled and fatigue softened conditions. Immediately prior to irradiation, the specimens were electropolished to remove surface damage caused by previous deformation. In all cases the same face was irradiated for a given crystal.

3.9 Electron Microscopy

Thin foils were prepared from sections cut parallel to the primary slip plane and from sections parallel to $(\bar{1}10)$, i.e. perpendicular to the primary plane. The crystals were oriented for cutting by reference to the surface slip lines which clearly traced the primary slip plane.

Sections were cut from near the center of the gauge length with a jeweller's saw and with the specimen firmly clamped in a specially designed brass "miter box". This was equipped with vertical guide slits for the saw blade at an angle to the tensile axis of the specimen appropriate for the particular orientation involved. Sections, about .060" thick, cut in this manner were then polished on successively finer grade emery paper, finishing with 600 grit paper, to produce smooth slices with parallel sides and approximately .050" thick. It was assumed that subsequent thinning would remove any damage remaining from the cutting and grinding operations.

These sections were further reduced in thickness by chemical polishing in a 50% nitric in water solution. A section was held at one corner by tweezers, which were suitably protected by Microstop, and suspended in the solution. A magnetic stirrer was used to provide

inued

rapid agitation of the solution. This method, accompanied by an occasional rotation of 180° of the specimen, resulted in a rapid and fairly uniform thinning of the section down to a thickness of about .005". At this thickness the amount of edge attack increased markedly so that continued thinning was accomplished by holding the specimen out of the solution and allowing the meniscus of liquid which formed to attack preferentially in the center region. Alternate periods of time in and out of the solution allowed the specimen to be thinned to an estimated .002" - .003" with the chemical polishing always being halted before any perforation of the surface resulted.

Final thinning was by electropolishing in a solution of 1/3 nitric acid, 2/3 methanol at 5 volts and a temperature of -30°C. At this point the edges of the specimen were protected with microstop and the standard "window" technique employed for the production of thin foils. Best results were obtained with chemically thinned specimens which were thick enough to allow at least 30 minutes of electropolishing prior to initial perforation. By this time the foil had been polished to an extremely bright smooth surface.

The thin foils were examined in a Siemens Elmiskop I electron microscope, operating at 100 kV. A double tilt specimen stage and cartridge were used which allowed a 20° tilt of the foil. Quantitative Burgers vector analyses were carried out on some of the specimens and in all cases every attempt was made to take low magnification photographs or higher magnification composites which would provide a truly representative picture of the dislocation microstructure developed.

3.10 Outline of the Experiment

Five single crystal specimens of identical orientation (for orientation see Figure 4.1) and 1" gauge length with 1/4" square crossection were produced.

Each of the five specimens were mounted and aligned in the fatigue adaptor and prestrained in tension to a nominal shear stress of 4.0 kg/mm^2.

One of the specimens was then softened at room temperature by fatigue cycling at constant plastic strain amplitude of $\pm$ .0025 for 1500 cycles. A second specimen was partially softened at the same temperature and strain amplitude for 40 cycles. Two specimens were cycled, each for 1500 cycles, at temperatures of -78°C and -26°C respectively, again at the same constant plastic strain amplitude of $\pm$ .0025. The remaining specimen was used to determine the structure developed during tensile deformation.

The cyclic stress-strain curves for the fatigue softened crystals were determined and the cumulative slip line topology produced by the tensile deformation and by the fatigue cycling was replicated and photographed for each specimen. Also, Laue back-reflection X-ray photographs were taken of the specimens after tensile deformation and after cycling and compared to those from the annealed, undeformed crystals.

Dislocation structures developed during deformation were investigated by transmission electron microscopy. Foils parallel to and perpendicular to the primary slip plane were examined from the specimen deformed in tension and from the specimen softened for 1500 cycles at room temperature. Foils were also examined parallel to the primary slip plane of the specimen cycled at -78°C.

CHAPTER 4

Experimental Results I - Macroscopic Observations

4.1 Introduction

For clarity, the macroscopic results including uniaxial and cyclic stress-strain response, slip line observations and X-ray results will be reported in this chapter separately from the electron microscopical observations of the dislocation structures. The latter will comprise Chapter 5.

The cyclic stress-strain response, particularly as a function of temperature, was an important part of the experiment and the softening curves were determined for crystals softened at three different temperatures. From these, the temperature dependence of the initial softening rate, defined in the present context as the percentage decrease in peak flow stress in the first 20 cycles, was determined.

The X-ray and slip line results reflect the overall change in the structure produced during deformation. The degree of asterism exhibited in the Laue spots is an indication of the nature of the lattice distortion produced, while slip line lengths are an indication of obstacle spacing in the crystal interior. These results can thus be correlated with other observations and are considered here qualitatively.

The orientation of the tensile axes of the specimens tested and the slip system notation used in this thesis are indicated in Figure 4.1.

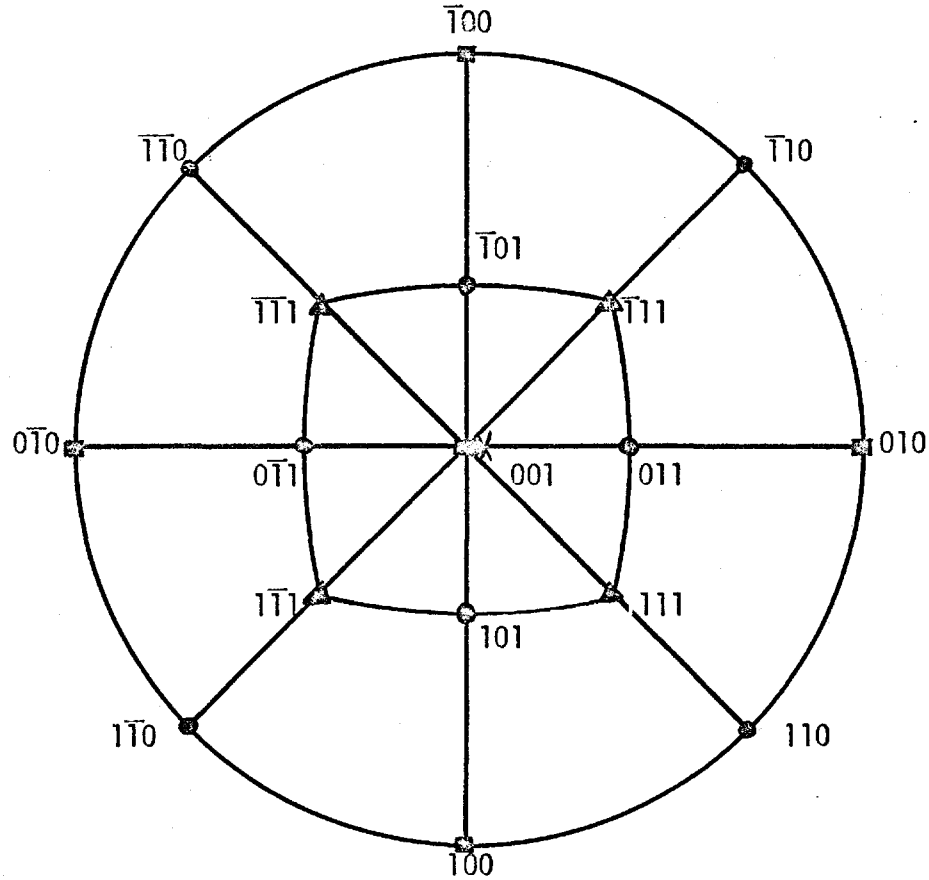

Tensile Axis of Specimens Denoted by "X"

		Schmid Factor
PRIMARY SYSTEM	$(111)\ [\bar{1}01]$	.46
COPLANAR SYSTEM	$(111)\ [0\bar{1}\bar{1}]$	.39
CROSS PLANE	$(1\bar{1}\bar{1})$	
CONJUGATE SYSTEM	$(\bar{1}\bar{1}1)\ [011]$	.39
CRITICAL SYSTEM	$(\bar{1}11)\ [101]$	.46
PRIMARY EDGE DIRECTION	$[1\bar{2}1]$	

FIGURE 4.1 - TENSILE AXIS OF SPECIMENS AND SLIP SYSTEM NOTATION

4.2 Uniaxial and Cyclic Stress-Strain Response

Each of the five single crystals were pulled in uniaxial tension to a nominal resolved shear stress of 4.0 kg/mm^2. A typical stress-strain curve is shown in Figure 4.2. The curve is as traced on the Instron chart recorder and is thus a plot of nominal resolved shear stress (calculated from the initial crossectional area) versus total strain.

The crossectional areas of the specimens were determined both before and after tensile deformation by measuring and calculating the crossectional areas at five different points along the gauge length and taking an average value. The true values of resolved shear stress were then calculated using the final areas. These results are summarized in Table 4.1.

Table 4.1

Crossectional Areas and Degree of Prestrain

Crystal	Initial Area (in^2)	Tensile Load (lb)	Final Area (in^2)	Resolved Shear Stress (kg/mm^2)
C1	.0583	720	.0505	4.61
C2	.0603	745	.0535	4.50
C3	.0598	728	.0523	4.54
C4	.0615	753	.0537	4.54
C5	.0620	764	.0544	4.54

The cyclic stress-strain curves for specimens C3, C5 and C4, fatigue softened for 1500 cycles at temperatures of 296°K, 247°K and 195°K respectively and for specimen C2, fatigue softened for 40 cycles at 296°K, are shown in Figure 4.3. These curves are plots of the peak resolved shear

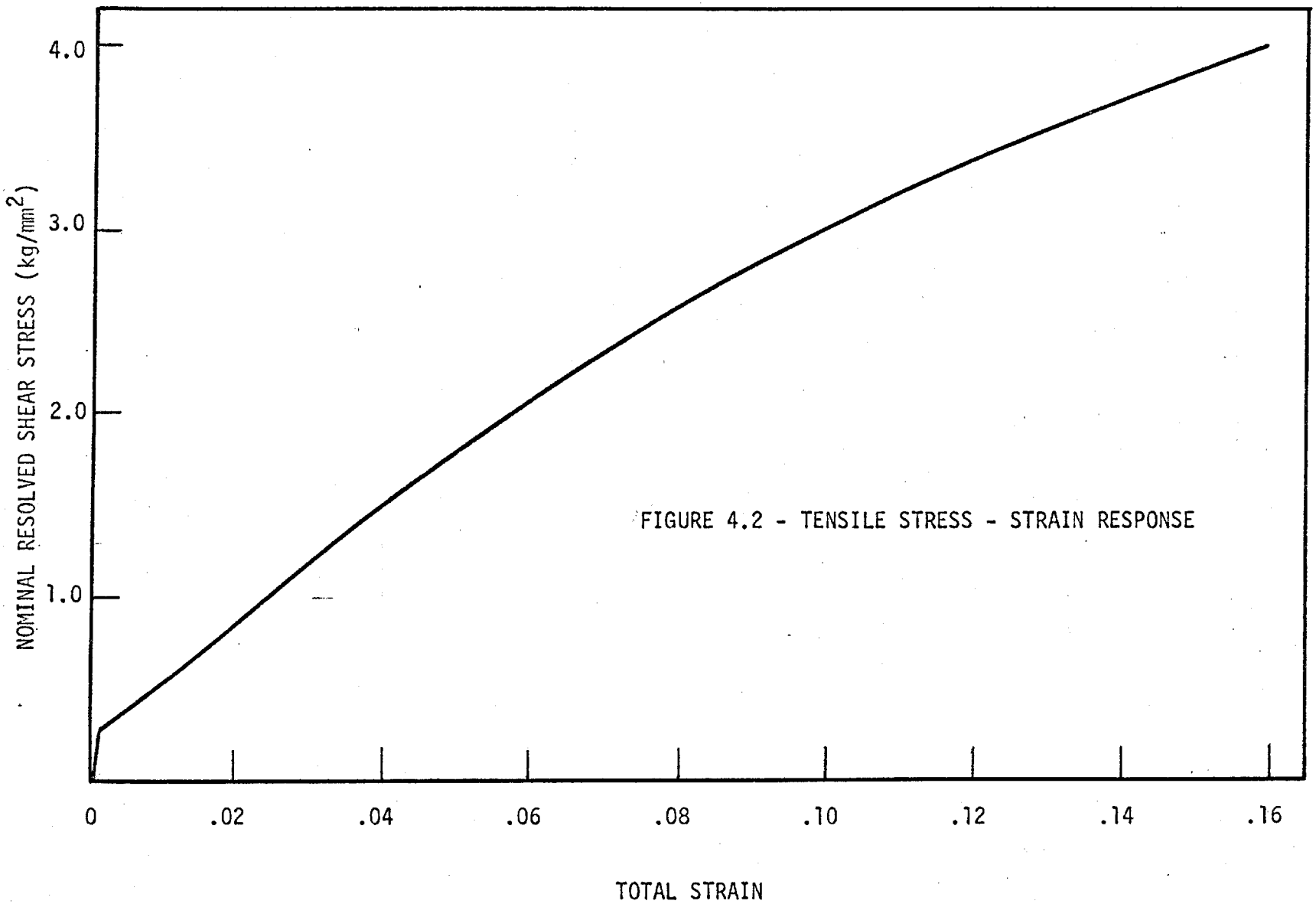

FIGURE 4.2 - TENSILE STRESS - STRAIN RESPONSE

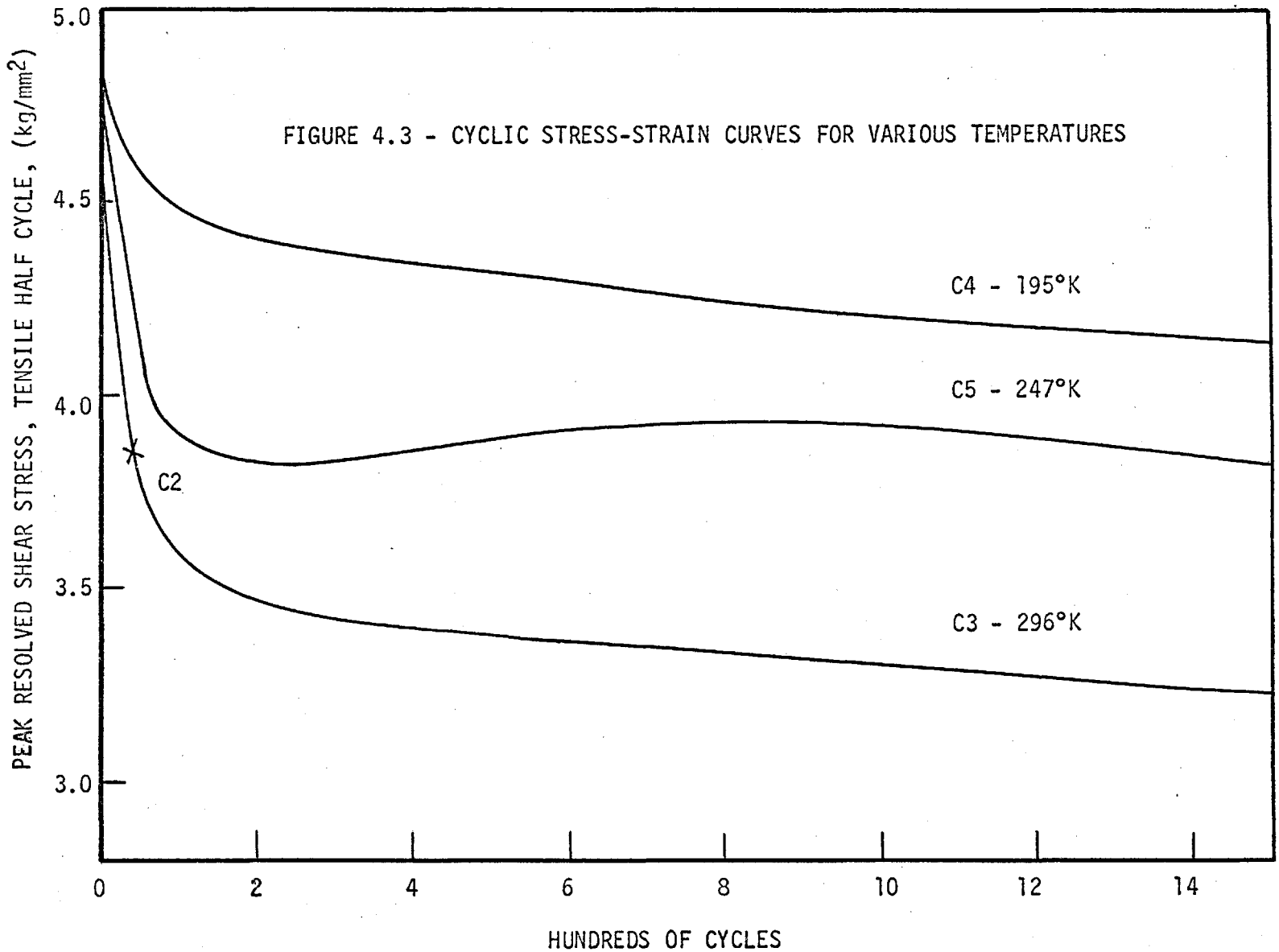

FIGURE 4.3 - CYCLIC STRESS-STRAIN CURVES FOR VARIOUS TEMPERATURES

stress during the tensile half cycles as a function of the number of cycles, during fatigue cycling at constant plastic strain amplitude of $\pm$ .0025.

The softening curves show a behaviour similar to that observed in thermal recovery (Byrne (1965)) in that they show an initial period of gradually decreasing softening rate and finally begin to level off and approach a saturation level of flow stress.

As the temperature is lowered, the softening rate decreases and it appears that a specimen will saturate at a higher stress level. It is possible however, that the latter effect is due to the much lower softening rate and that eventually, provided fatigue fracture did not occur first, the same stress level would be attained for all temperatures.

The first 400 cycles of the softening curves are shown expanded in Figures 4.4, 4.5 and 4.6 for cycling at 296°K, 247°K and 196°K respectively. In this case the curves are normalized, for easy comparison, by plotting the peak resolved shear stress as a fraction of the peak resolved shear stress attained during the first tensile half-cycle. Also plotted, as a broken line, is the peak resolved shear stress during the compressive half-cycles, again normalized with respect to the first tensile half cycle. For C3, at 296°K, the Bauschinger effect is seen to gradually decrease to zero with continued cycling, as would be expected. At the two lower temperatures, however, the behaviour is more complex. Here, the effect decreases quickly to zero and changes sign before again approaching zero.

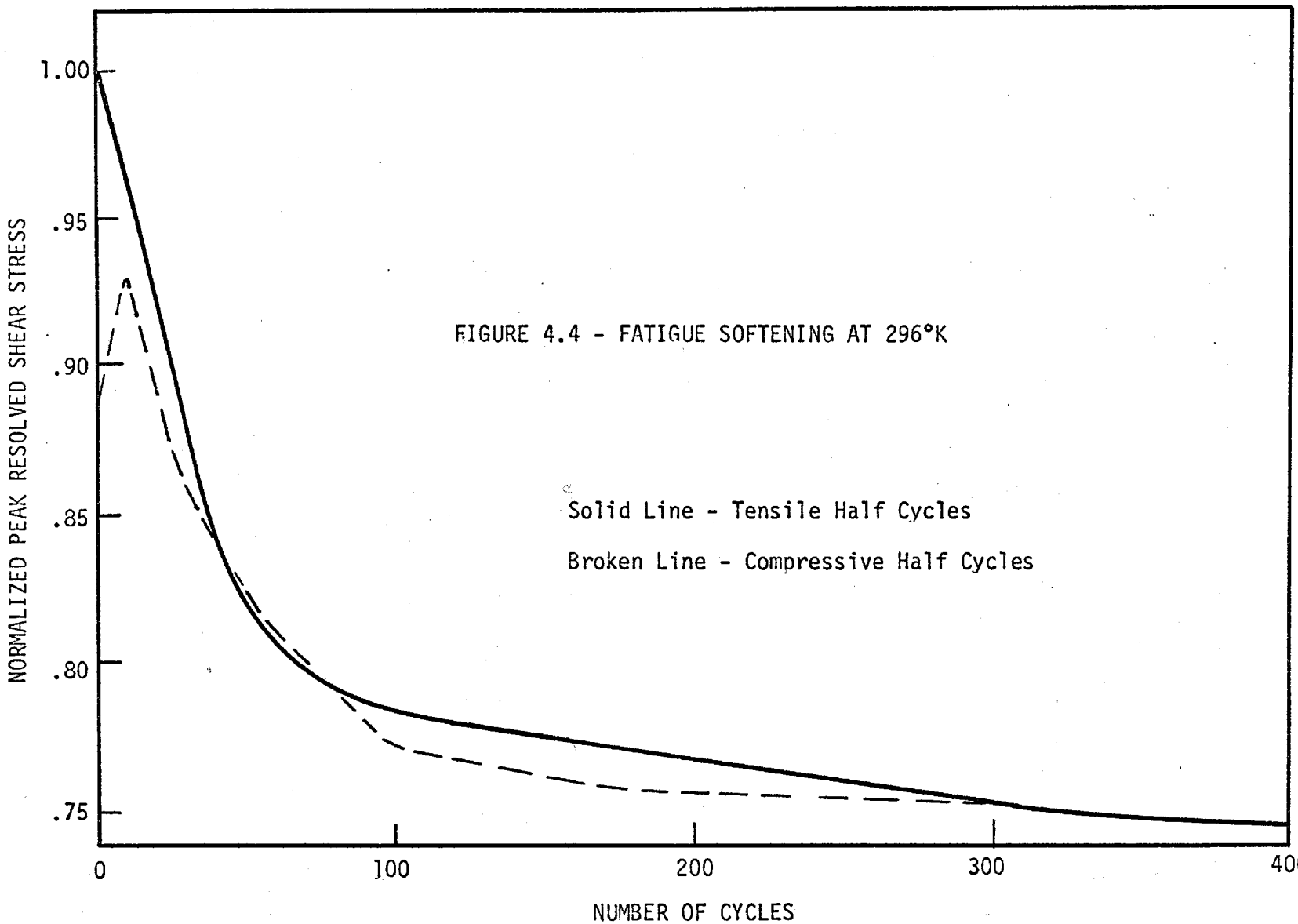

FIGURE 4.4 - FATIGUE SOFTENING AT 296°K

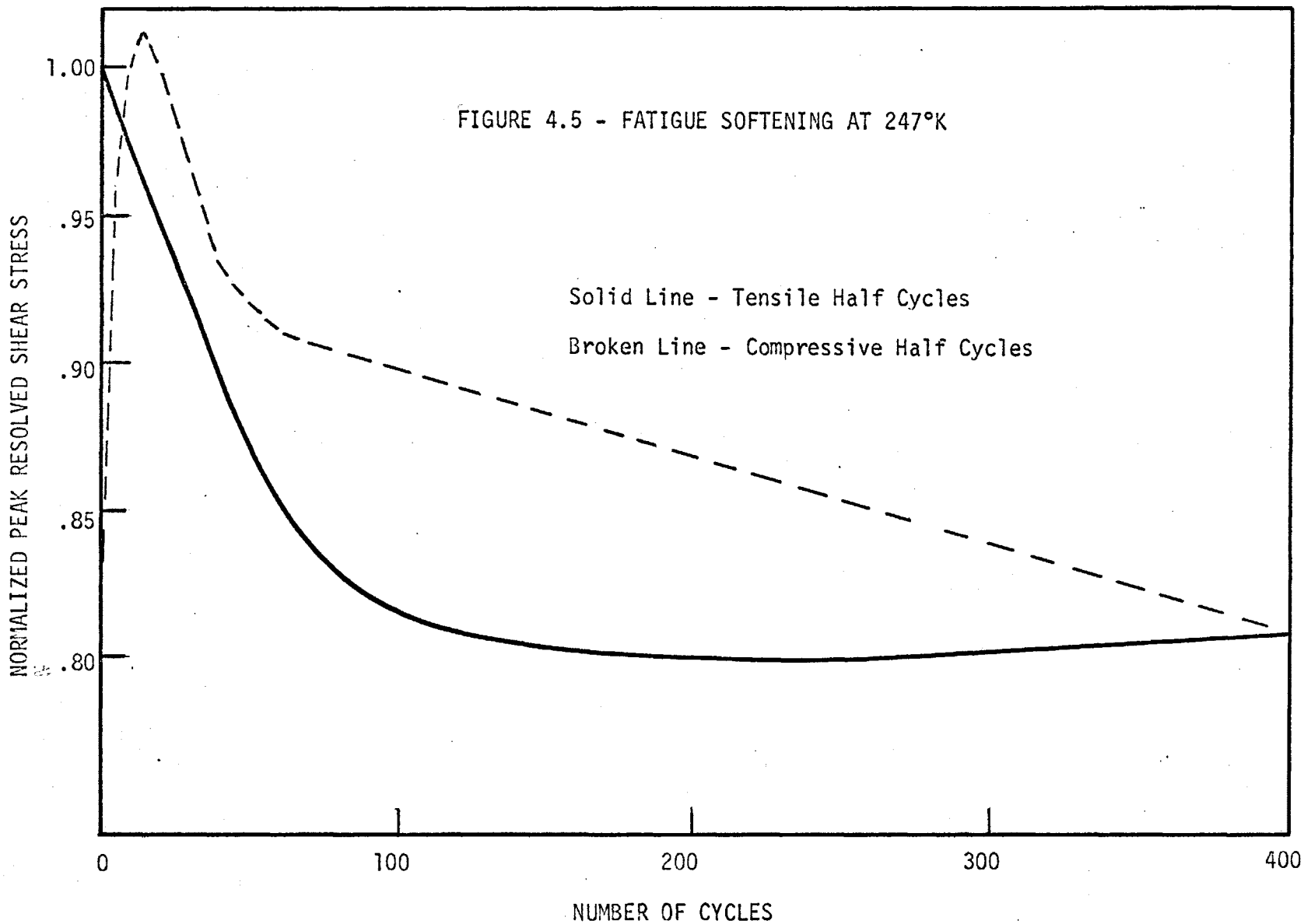

FIGURE 4.5 - FATIGUE SOFTENING AT 247°K

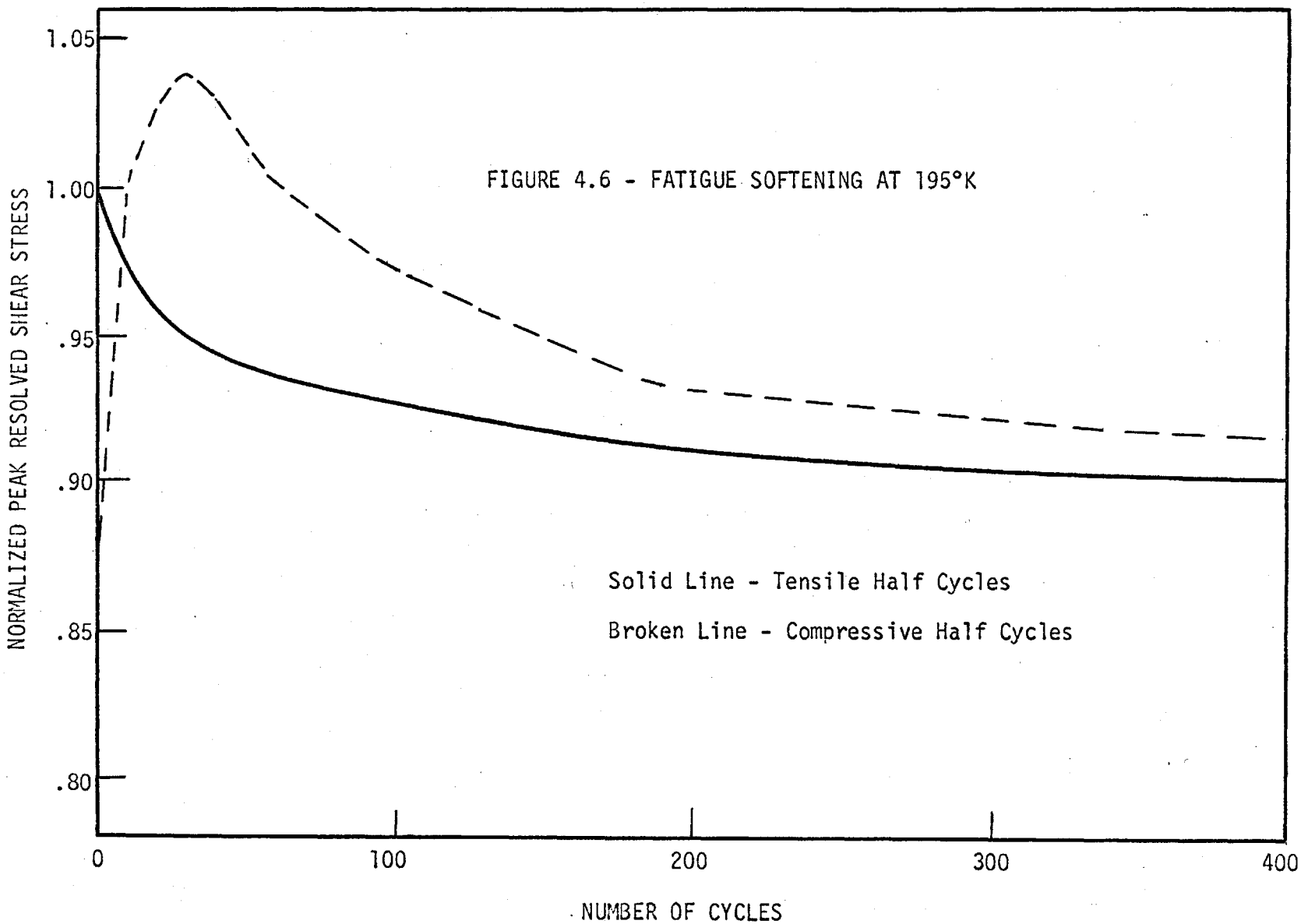

FIGURE 4.6 - FATIGUE SOFTENING AT 195°K

4.3 Temperature Dependence of Softening Rate

As mentioned previously with respect to Figure 4.3, the softening rate decreases with decreasing temperature. For the purpose of comparison, the softening rate is defined as the percentage decrease in peak resolved shear stress in the first 20 cycles. Thus, the measured softening rates at 296°K, 247°K and 195°K respectively are 7.15%, 5.3% and 4.1% (See Figure 6.1)

4.4 X-ray Results

In figure 4.7 are reproduced the Laue back reflection X-ray photographs taken at various stages in the deformation history of specimen C3. The results for the other specimens are very similar and thus will not be included.

In figure 4.7 (a), from the annealed undeformed crystal, the Laue spots are sharp and exhibit very little asterism, or streaking. The splitting of many of the spots, however, indicates the existance of some degree of substructure, i.e. low angle boundaries.

Figure 4.7 (b), after tensile deformation, shows increased splitting of the Laue spots and considerable streaking of the stronger spots. This is indicative of and consistent with the lattice misorientations and distortion caused by this mode of deformation.

In figure 4.7 (c), after fatigue softening for 1500 cycles at room temperature, the Laue spots exhibit somewhat less asterism and less splitting than was the case after tensile deformation. Thus, it appears that the lattice distortion produced in the tensile deformation decreases during softening.

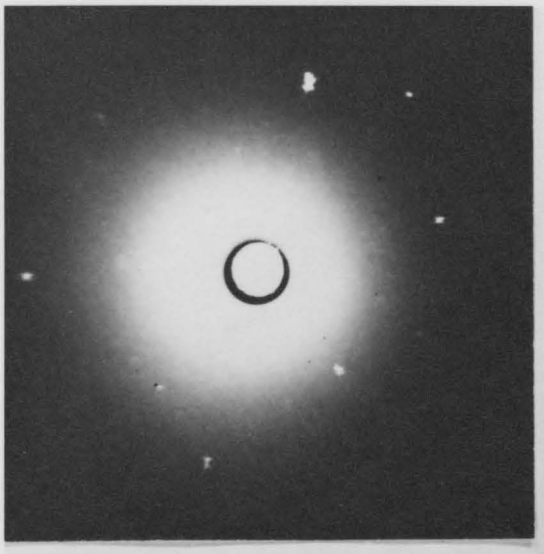

(a) - annealed, undeformed

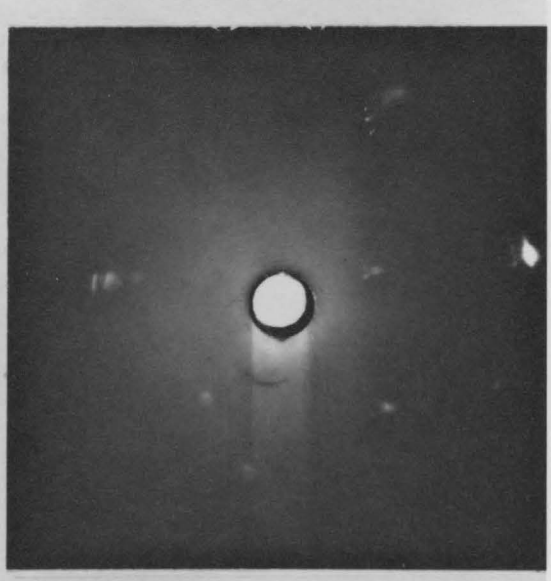

(b) - pulled in tension

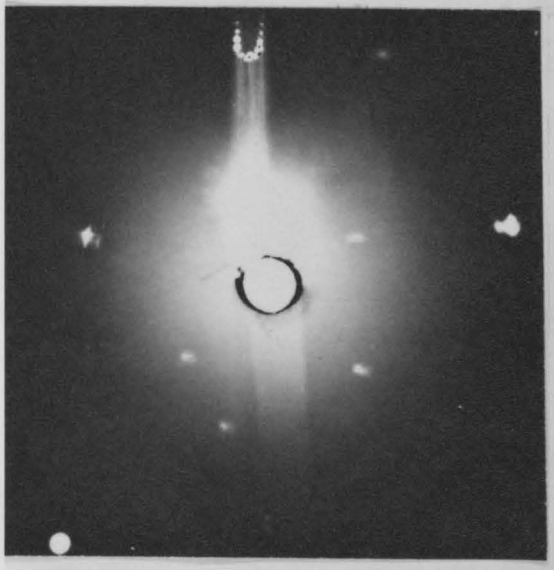

(c) - fatigue softened 1500 cycles

FIGURE 4.7 - LAUE BACK REFLECTION PHOTOGRAPHS FROM SPECIMEN C3

4.5 Slip Line Results

No quantitative slip line measurements were attempted but the general trend of slip line development can be seen in Figure 4.8. All photographs were taken directly from the specimen surfaces with the exception of figure 4.8 (a) which is from a shadowed replica.

The main features to note are the long, fairly coarse slip lines developed during tensile deformation (Figure 4.8 (a)) and indicating little evidence of secondary slip. Figures 4.8 (b) and 4.8 (c) represent the cumulative slip line development after fatigue softening at room temperature for 40 cycles and 1500 cycles respectively with the slip lines becoming finer and of shorter length. Again, there is no evidence of secondary slip and the slip lines are uniformly distributed over the specimen surface. Specimen C5, after fatigue cycling at 247°K for 1500 cycles, was repolished and cycled at room temperature for an additional 3000 cycles. As seen in figure 4.8 (d), persistent slip bands, or bands into which all resolvable slip is concentrated, have formed. Note also the cross-slip traces connecting separate bands.

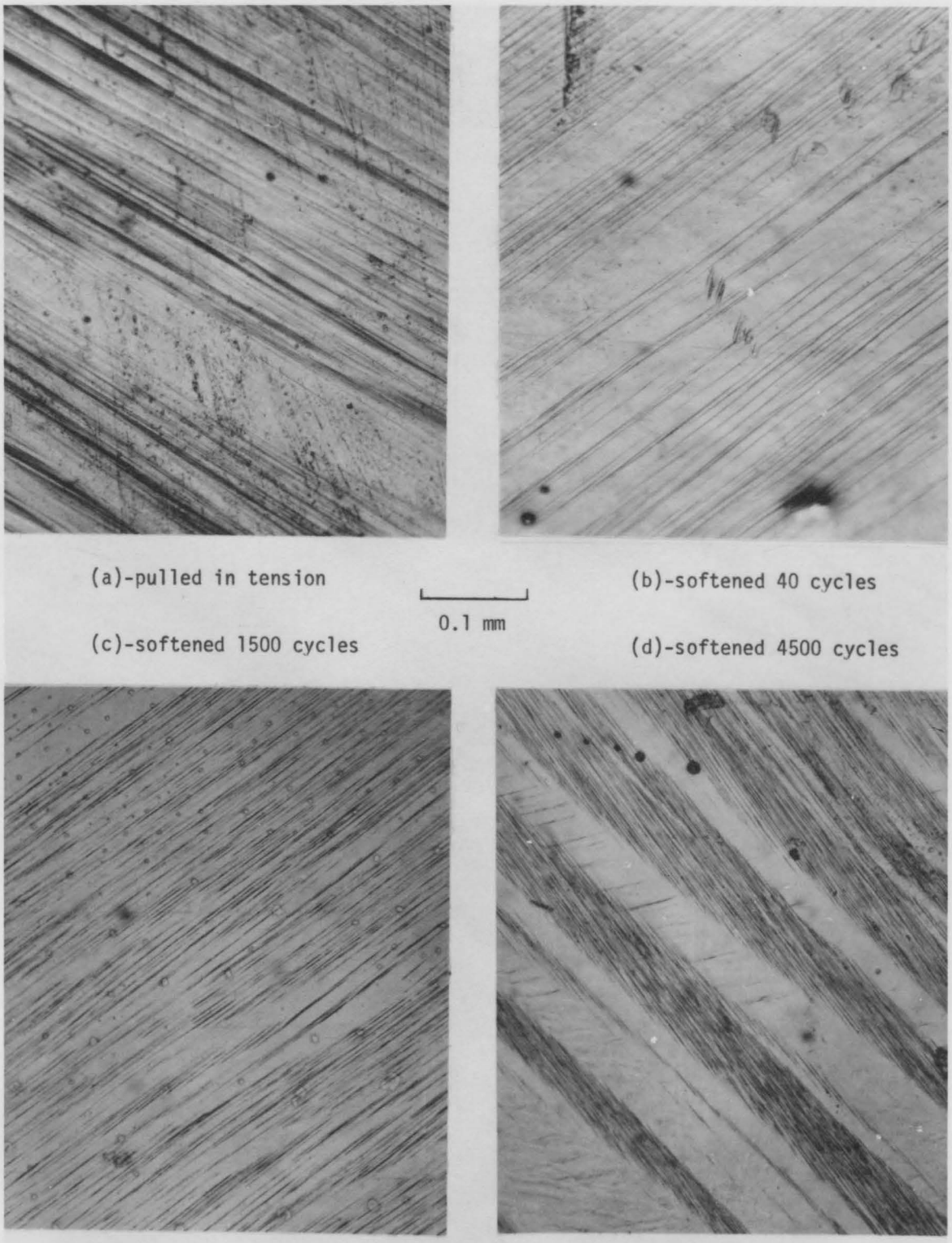

FIGURE 4.8 - SLIP LINE DEVELOPMENT DURING DEFORMATION

CHAPTER 5

EXPERIMENTAL RESULTS II - ELECTRON MICROSCOPY

5.1 Introduction

A major part of the investigation was concerned with the use of contrast experiments in the electron microscope to determine the nature of the detailed dislocation substructure developed during the tensile deformation and during the subsequent fatigue softening. In order to establish a comprehensive view of the dislocation microstructure in three dimensions, foils were produced from sections approximately parallel to the primary slip plane, (111), and perpendicular to the primary plane, i.e. parallel to $(\bar{1}01)$, in the case of the specimen deformed in tension and for the specimen fatigue softened at room temperature. A (111) foil was examined for the specimen fatigue softened at a temperature of 195°K.

Several Burgers vector analyses were carried out to determine the nature and distribution of the dislocations present. For this purpose the standard g.b=0 criterion for dislocation invisibility (Hirsch, Howie, Nicholson, Pashley, Whelan (1965)) was followed.

The following micrographs are grouped according to the deformation mode each exemplifies. Each micrograph is chosen as representative from the large number of photographs taken from each foil. In addition to the detailed analysis of the dislocation structure using the double tilt stage to define suitable contrast conditions, a number of composite micrographs have been included to illustrate the general scale and arrangement of the

dislocation substructure.

5.2 Dislocation Structure During Uniaxial Tension

5.2.1 Electron Micrograph #1

Resolved Shear Stress: 4.61 kg/mm^2

Foil Normal: [111]

A low magnification composite which shows the general dislocation structure developed parallel to the primary slip plane in early stage III of tensile deformation. The main feature is the formation of a loose cell structure. Although there is a definite predominance of cell walls lying along the primary edge direction, $[1\bar{2}1]$, and along the intersection of the primary plane with the critical plane, $[0\bar{1}1]$, and with the conjugate plane, $[\bar{1}10]$, the orientation of the cell walls are not well defined over long distances.

The walls themselves are composed of loose tangles of dislocations while the cell interiors are essentially dislocation free except for numerous dipole loops.

#1

5.2.2 Electron Micrograph #2

Resolved Shear Stress: 4.61 kg/mm^2

Foil Normal: [111]

This is a higher magnification composite showing in more detail the dislocation arrangement in the bundles and again, the preferential alignment along $[1\bar{2}1]$ and $\langle\bar{1}10\rangle$ type directions. Contrast experiments were performed in this region of the foil as discussed in Micrograph #3.

#2

5.2.3 Electron Micrograph #3

Resolved Shear Stress: 4.61 kg/mm^2

Foil Normal: [111]

This pair of micrographs illustrates the change in contrast observed on tilting the region shown in micrograph #2. Under the operating reflection g = $0\bar{2}2$, most of the $\frac{a}{2}$ [110] dislocations, including the primaries are in contrast. Under the operating reflection g = $1\bar{1}1$, the primary $\frac{a}{2}$ [$\bar{1}$01] is invisible and the number of dislocations in the network which remain visible is considerbly reduced.

Of the dislocations remaining in contrast, the density remains more or less uniform along all directions of the network, indicating that all the bundles are composed of the same proportion of secondaries. Some of the secondaries visible are fairly long so that, assuming they lie in the plane of the foil, they must be $\frac{a}{2}$ [0$\bar{1}$1] dislocations of the coplanar or critical slip systems ($\frac{a}{2}$ [$\bar{1}$10] dislocations are very lightly stressed on all systems).

Most of the dipole loops visible under g = $0\bar{2}2$ lie along [$1\bar{2}1$], i.e. at A, and are out of contrast under g = $1\bar{1}1$. They are thus, as expected, primary edge dipoles and appear within the bundles as well. Several primary screw dislocations, i.e. at points B, are evident.

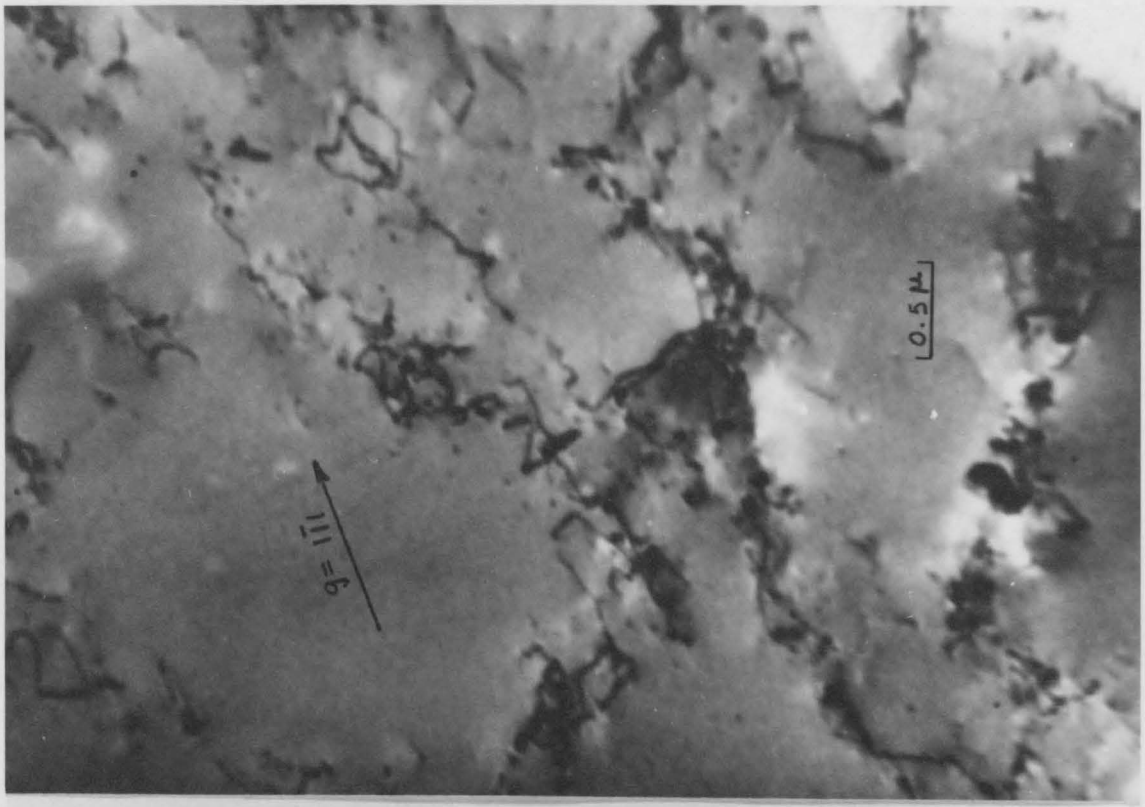

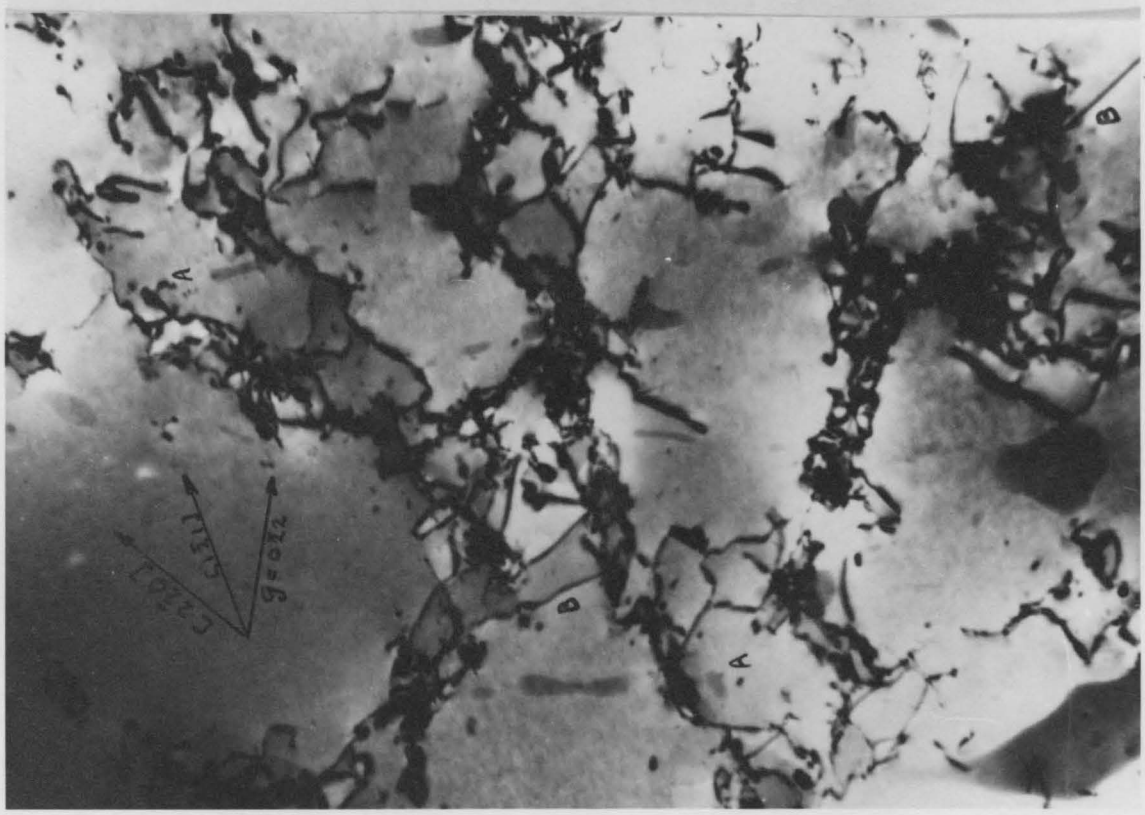

#3

5.2.4 Electron Micrographs #4 and #5

Resolved Shear Stress: 4.61 kg/mm^2

Foil Normal: [$\bar{1}$10]

These micrographs illustrate the structure observed in sections cut perpendicular to the primary slip plane, i.e. parallel to ($\bar{1}$10), and show the two salient aspects of the dislocation structure.

The structure contains dense bands of dislocations lying along the trace of the primary plane and separating regions of relatively low dislocation density. This implies that the dislocation structure on the primary plane is effectively two-dimensional in these regions. Some of the bands are seen to divide regions of different contrast which indicates the existence of misorientations, or lattice rotation, about the primary trace.

As can be seen in some areas of micrograph #4 and particularly in micrograph #5, a second feature of the structure are dense walls of dislocations orthogonal to the primary slip trace. These walls form occasionally along the traces of the critical and conjugate slip planes.

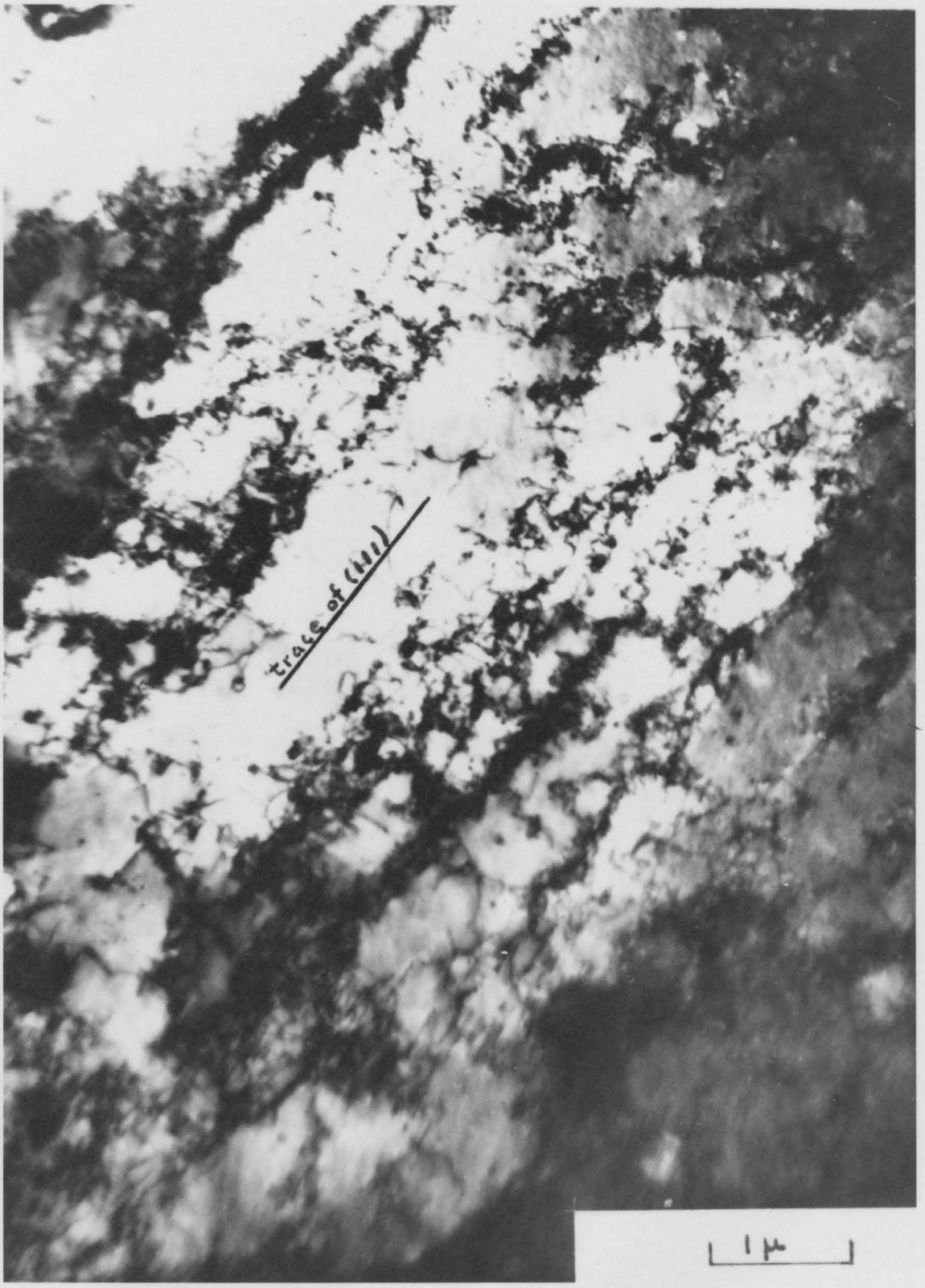

#4

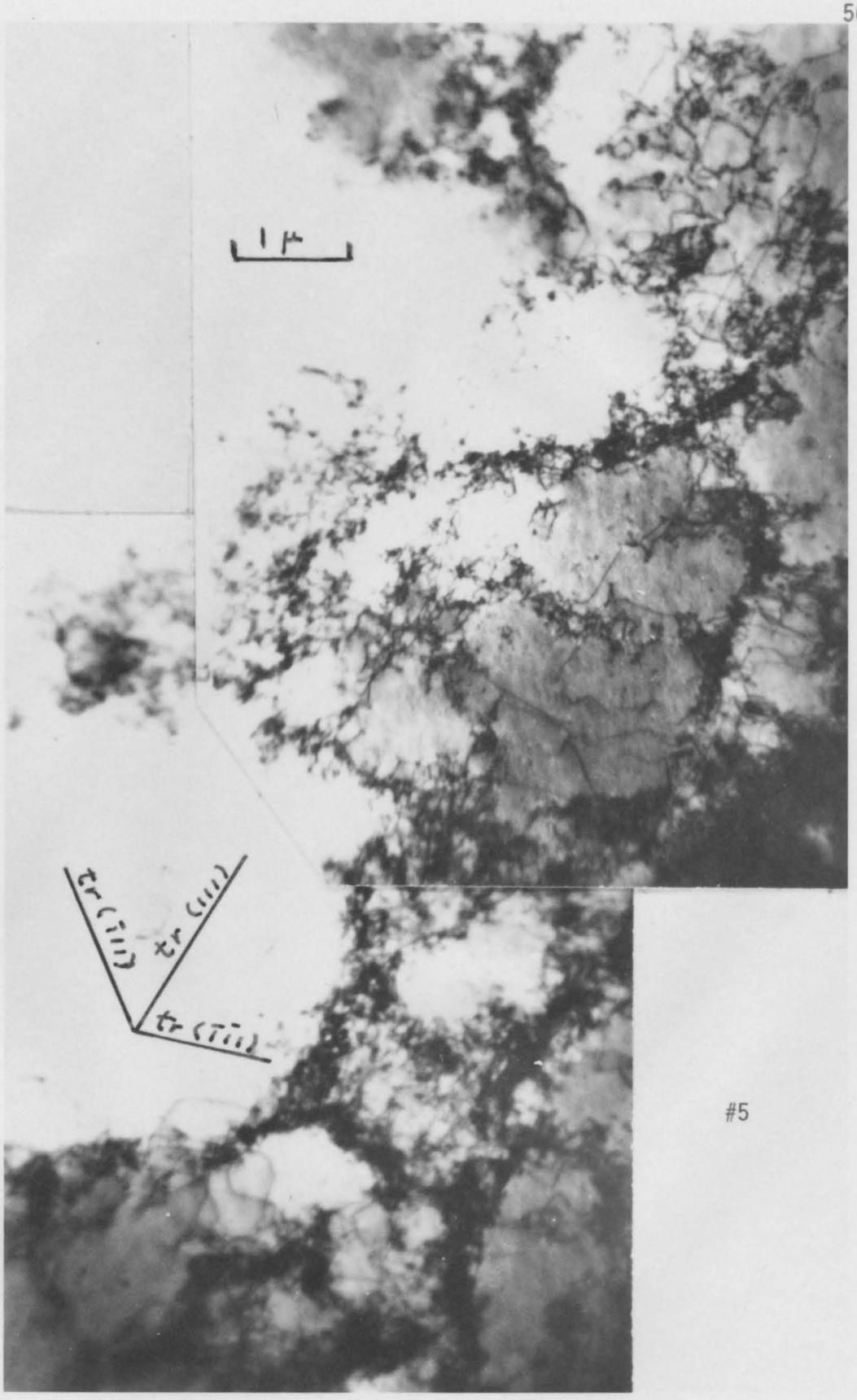

#5

5.3 Dislocation Structure After Fatigue Softening

5.3.1 Electron Micrographs #6 and #7

Softening Temperature: 296°K

Strain: 1500 cycles

Foil Normal: [111]

These two low magnification photographs show the typical cell structure which is developed parallel to the primary slip plane during fatigue softening at room temperature. The network formation is not quite "complete" in that some of the cells are not entirely enclosed. There is a marked tendency for cell walls to align along $[0\bar{1}\bar{1}]$ and $[\bar{1}10]$, the traces of the critical and conjugate slip planes respectively.

The scale of the network is similar to that developed during pre-strain although the walls appear more narrow and more densely packed. Some of the walls, particularly those along the critical trace, appear tightly packed with primary edge dipoles. In other areas the dislocations are in tangled mats, less tightly packed and of broader extent than the walls.

Of the isolated long lengths of dislocations in these micrographs, assuming them to lie in the plane of the foil, many are primary edges. Primary screw dislocations and coplanar $\frac{a}{2}[0\bar{1}1]$ edge and screw dislocations are also evident.

#6

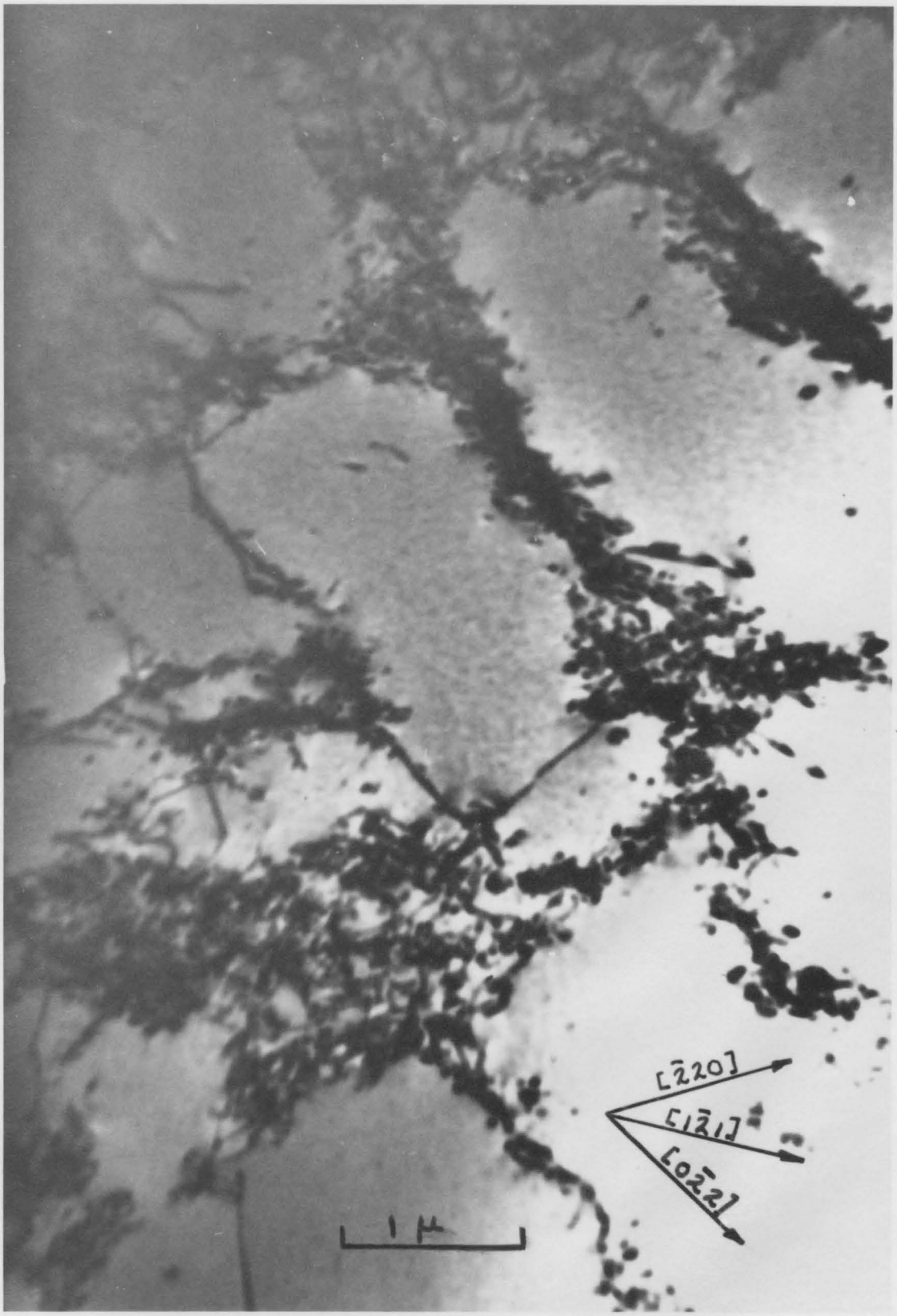

#7

5.3.2 Electron Micrograph #8

Softening Temperature: 296°K

Strain: 1500 cycles

Foil Normal: [111]

This is a larger magnification photograph showing some of the detail of the loose dislocation tangles. A large number of dipole loops, mainly primary edges but also a number of $\frac{a}{2}[0\bar{1}1]$ coplanar edges, are evident both in the center of the tangles and at the extremities. There are also a large number of small loops in the relatively clear areas between the tangles. Many of the longer dislocations appear to be primary or coplanar $\frac{a}{2}[0\bar{1}1]$ screw dislocations.

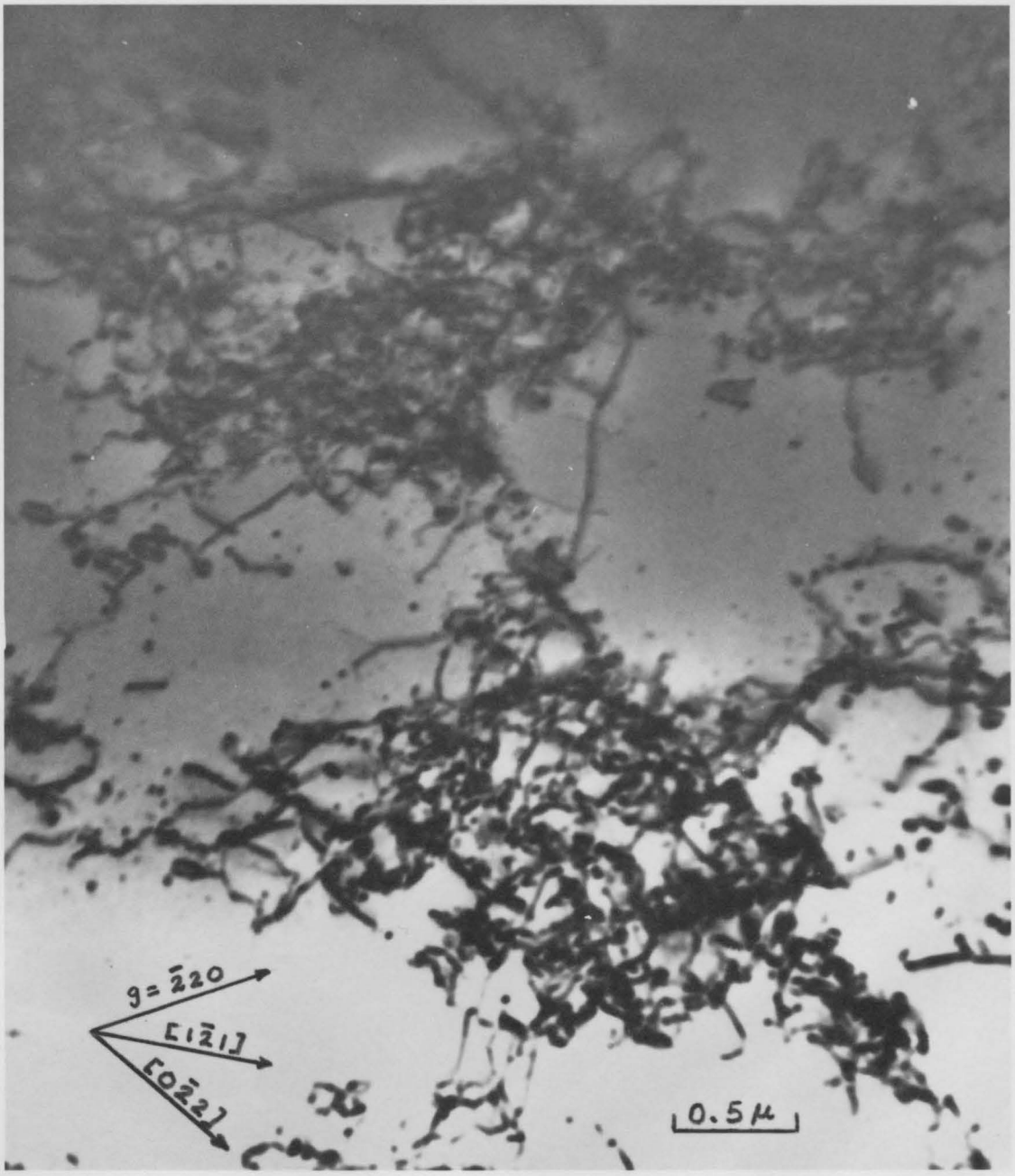

#8

5.3.3 Electron Micrograph #9

Softening Temperature: 296°K

Strain: 1500 cycles

Foil Normal: [111]

This Burgers vector pair reveals the large dipole content of the cell walls. Under the operating reflection g = $20\bar{2}$, primary dislocations are in contrast and a large number of primary edge dipoles can be seen packed tightly along the critical trace, $[0\bar{1}1]$. In the region at the top of the photograph a number of loops are evident near the tangle but cannot be distinguished within the tangle.

With the operating reflection g = $1\bar{1}1$ the primary Burgers vector becomes invisible and the resulting braids reveal only a small fraction of the original dislocation density. A small number of coplanar loops, visible under this reflection, can be seen particularly at the top of the photograph. Apart from the primary loops, the braids are seen to consist of coplanar loops, some long heavily jogged dislocations which are probably coplanar or critical $\frac{a}{2}[0\bar{1}1]$ screws and unidentified secondary debris.

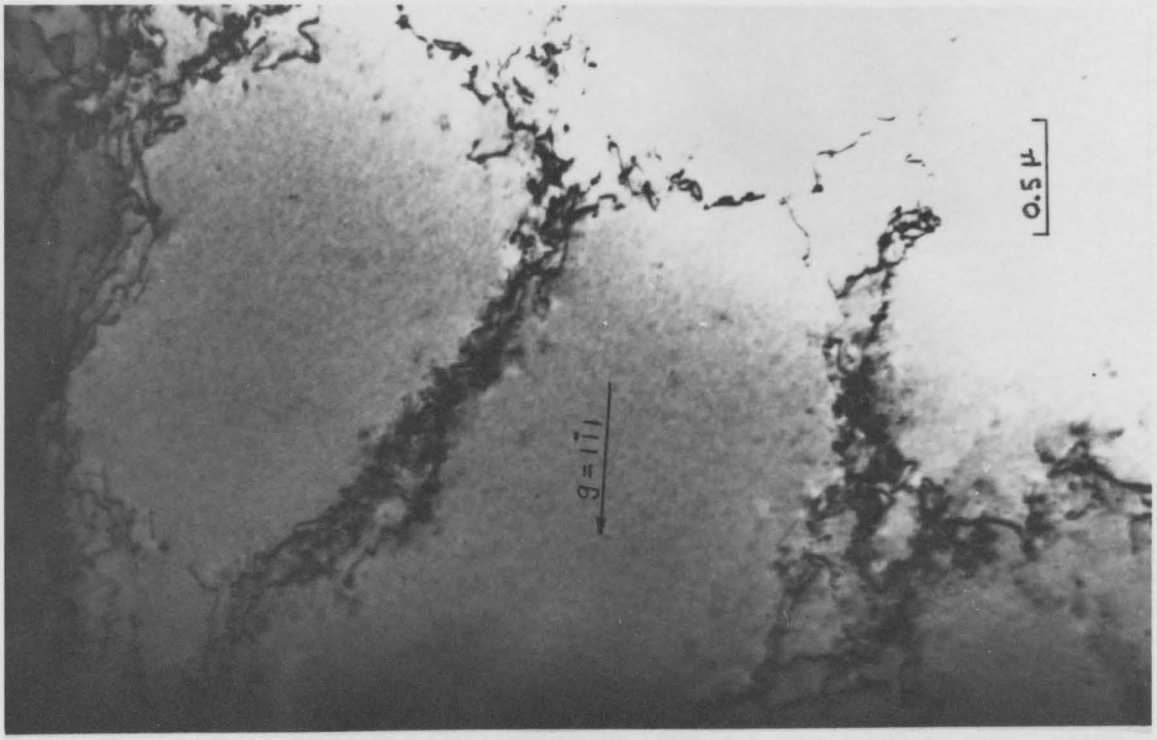
g=1$\bar{1}$1
0.5 μ


g=202
[$\bar{1}$01]
[$\bar{1}$2$\bar{1}$]

5.3.4 Electron Micrograph #10

Softening Temperature: 296°K

Strain: 1500 cycles

Foil Normal: $[\bar{1}10]$

Micrograph #10 is a low magnification composite showing the uniform and well defined cell structure observed in sections perpendicular to the primary plane. The walls are aligned preferentially along the trace of the critical plane with some short segments along the traces of the primary and conjugate planes. The segments along the critical trace as well as the segments along the same trace in sections parallel to the primary plane can thus be parts of two-dimensional walls lying in the critical plane. The critical plane makes an angle of approximately 35° to the present foil so that, because of the thinness of the foil, these walls would appear narrow.

This composite shows a uniformity of contrast from one cell to another and over a large area of the foil. Thus there are no misorientations across the cell walls which indicates that they consist of approximately equal numbers of dislocations of opposite sign. This is consistent with the large concentration of dipoles observed in the walls.

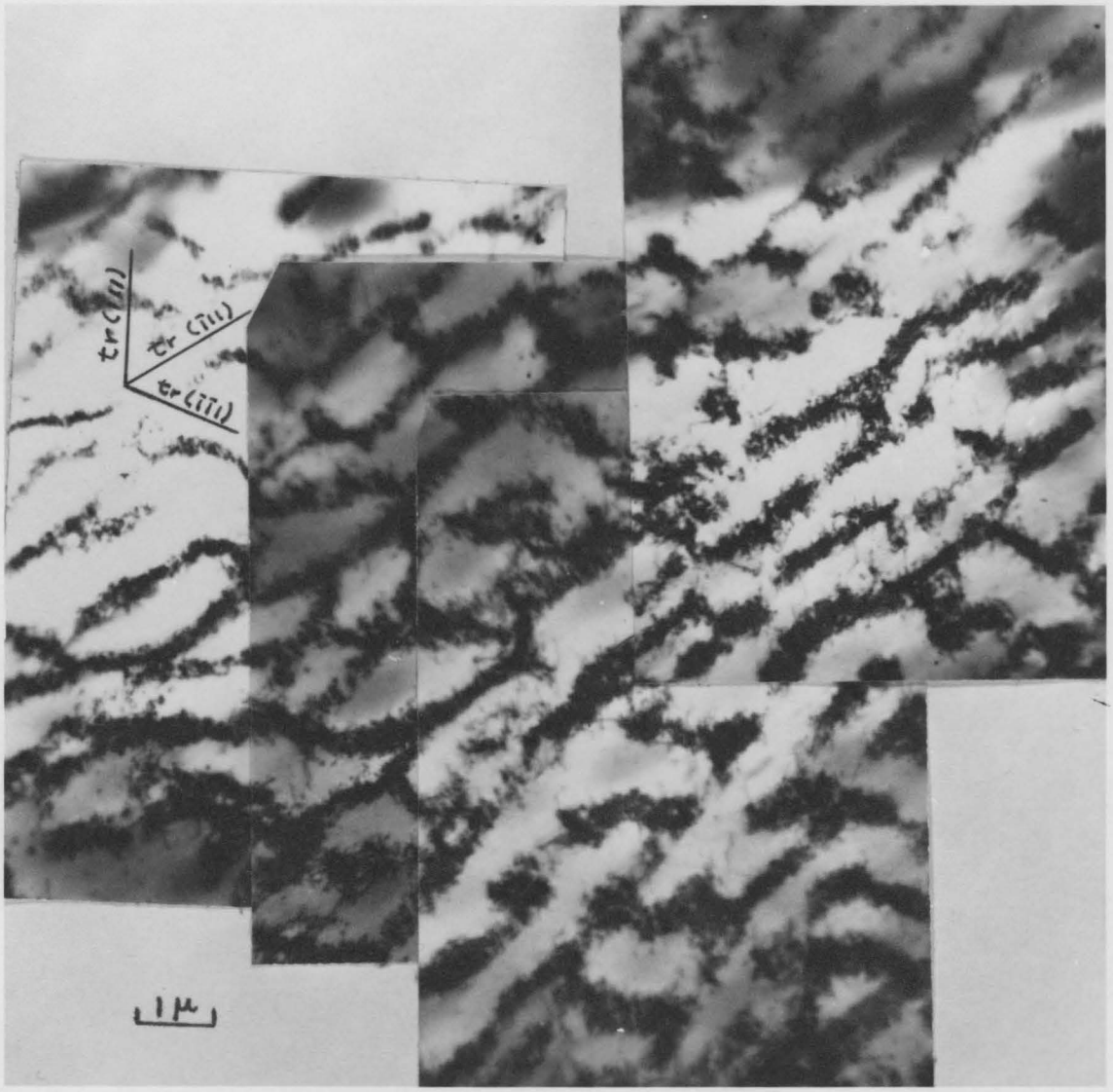

#10

5.3.5 Electron Micrograph #11

Softening Temperature: 296°K

Strain: 1500 cycles

Foil Normal: $[\bar{1}10]$

This is a higher magnification photograph showing the cell walls in more detail. Although no Burgers vector analysis was done and the traces of the primary and conjugate planes could not be unambiguously distinguished, certain features are evident. In particular, a large number of short parallel dislocations tranverse to the wall directions can be seen. Assuming that the primary trace is as marked, it is interesting to speculate that this transverse dislocation structure is in fact composed of primary edge dipoles packed on parallel slip planes.

#11

5.4 Dislocation Structure After Fatigue Softening at 195°K

5.4.1 Electron Micrograph #12

Softening Temperature: 195°K

Strain: 1500 cycles

Foil Normal: [111]

The structure developed during fatigue softening at 195°K is qualitatively similar to that found after cycling at room temperature. As seen in this photograph, the same basic cell structure is evident, with preferential alignment of the cell walls along the directions $[\bar{1}10]$, $[1\bar{2}1]$ and $[0\bar{1}1]$, and the scale of the network has decreased somewhat. (Compare micrograph #7).

Again, the walls appear densely packed with mainly primary edge dipoles and a large number of primary and coplanar $\frac{a}{2}[0\bar{1}1]$ screw dislocations are evident. Many of the primary screws are jogged and in some cases (at points marked A) are in the process of dipole formation by jog dragging.

#12

CHAPTER 6

DISCUSSION

6.1 Discussion of Macroscopic Results

As detailed in chapter 4, copper single crystals prestrained in tension to a shear stress of approximately 4.5 kg/mm^2 soften when fatigued at constant plastic strain amplitude of $\pm$ .0025. Both the rate of softening and the amount of softening, i.e. the reduction in peak flow stress attained at saturation, depend strongly on temperature, decreasing as the temperature decreases.

In Figure 6.1 the temperature dependance of the softening behaviour is compared to that exhibited by related parameters. In Figure 6.1 (a) the natural logarithm of the softening rate, defined in chapter 4 as the percentage decrease in peak flow stress in the first 20 cycles, is plotted together with ln τ_{III} as a function of temperature. τ_{III} is the shear stress defining the beginning of stage III in uniaxial tension and is usually associated with the onset of large scale thermally activated cross-slip. The values of τ_{III} have been taken from the data of Mitchell and Thornton (1963) and relate to copper single crystals of similar orientation to those tested in the present experiment. The slopes of the two lines agree to within 50% which, in view of the errors involved in defining and measuring τ_{III} (Mitchell and Thornton reported two values, 2.0 kg/mm^2 and 3.1 kg/mm^2, for the same orientation crystal at room temperature), is considered adequate for a correlation to be made between the rate controlling process in fatigue softening and the fundamental process

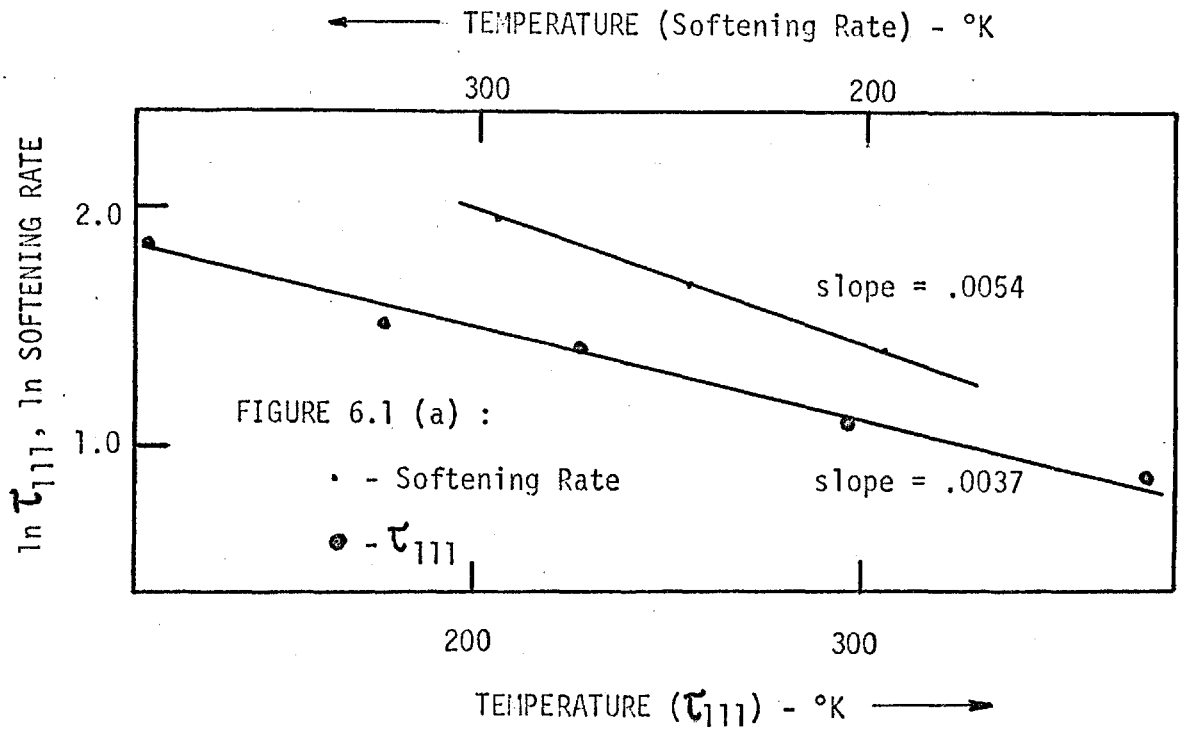

FIGURE 6.1 (a) :

• - Softening Rate

⊙ - τ_{111}

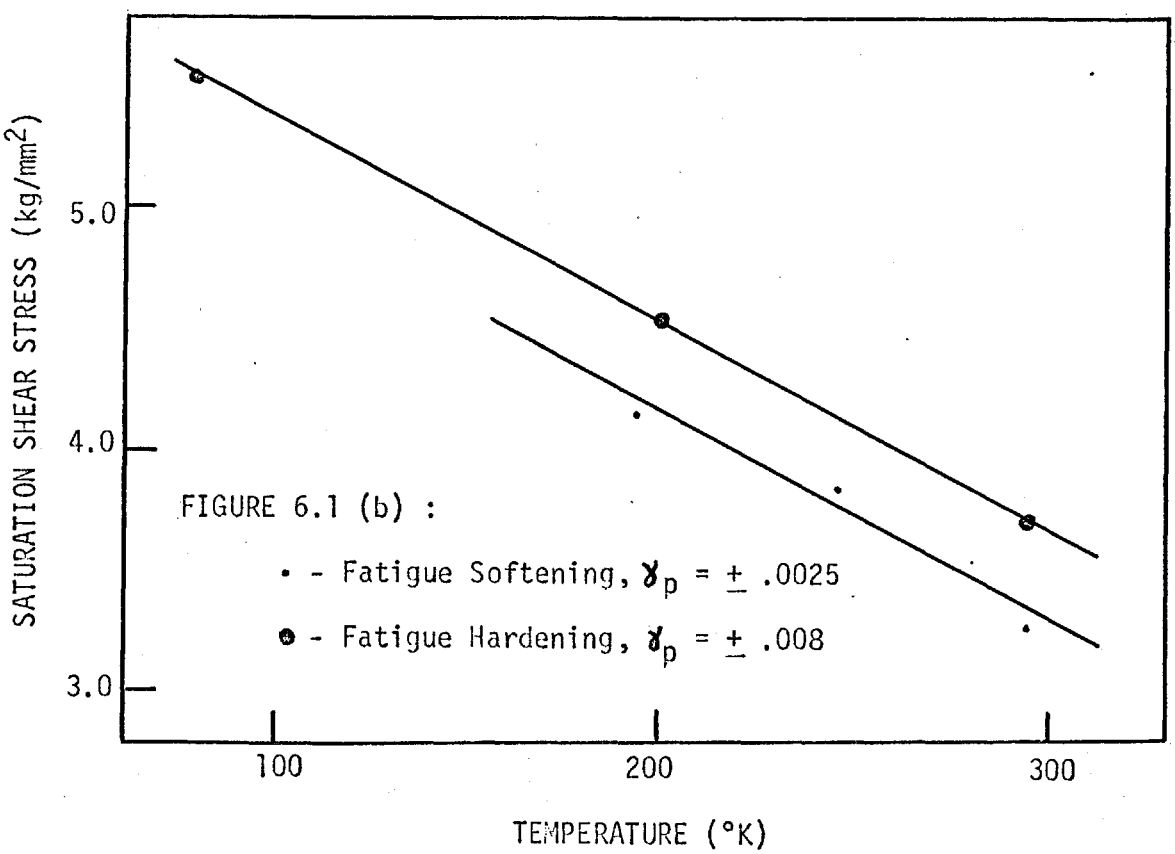

FIGURE 6.1 (b) :

• - Fatigue Softening, $\gamma_p = \pm .0025$

⊙ - Fatigue Hardening, $\gamma_p = \pm .008$

determining τ_{111}, namely cross-slip. A kinetic analysis of the softening curves is beyond the scope of this thesis and no attempt was made to relate either slope of Figure 6.1 (a) to an activation energy (the activation energies for the softening process and for cross-slip are stress dependant so that an analysis in these terms would require a knowledge of the internal stress distributions).

The temperature dependance of the saturation stress attained during fatigue softening and during fatigue hardening is compared in Figure 6.1 (b). The hardening data is from Feltner (1965) who used copper single crystals of [011] orientation. Although his lowest plastic strain amplitude used was $\pm$ .008 (tests at higher strain amplitude exhibited very similar behaviour but at higher stresses), it is reasonable to conclude that the saturation stresses in hardening and softening depend on temperature in the same way. Also, the result reported by Feltner (1967) that copper polycrystals cycled at the same strain amplitude and temperature soften or harden to the same saturation stress appears to be valid in the case of single crystals.

During fatigue softening, the large Bauschinger effect exhibited on the first strain reversal gradually decreases with continued cycling and disappears after approximately 300 cycles (see Figure 4.4). Thus, it appears that the polarization of the dislocation structure developed by the prestrain, which gives rise to backstresses that assist the reverse motion of dislocations when the direction of loading is reversed, is gradually reduced and finally eliminated during cycling. Feltner (1967) observed the same effect in polycrystals of copper but found that in in the case of Cu - 7.5% Al, a planar slip mode material, that the

Bauschinger effect remained with continued hardening or softening. It would seem, therefore, that cross-slip is a probable mechanism for the rearrangement of a structure into one which is symmetric with respect to reverse loading.

A basic rearrangement of the overall structure is also evident from the X-ray results (Figure 4.7). The asterism exhibited in the Laue spots indicates that after tensile deformation, considerable lattice distortion, caused by strain gradients in the lattice, exists. During fatigue softening, the strain gradients are relieved and the Laue spots from the softened structure show decreased asterism.

Slip line evidence (Figure 4.8) indicates that the dislocation structure developed by softening to saturation is mechanically extremely unstable. After 1500 cycles (Figure 4.8 (c)), fine slip lines are distributed uniformly over the surface of the specimen. An additional 3000 cycles (Figure 4.8 (d)) results in the concentration of slip into broad bands, separating slip-free regions and joined by prominent slip on the cross-slip system. These coarse slip bands are similar to the persistent slip bands observed by Watt (1967) on fatigue hardened copper single crystals (in Watt's case, slip was more concentrated and the slip bands were more closely parallel to the individual slip lines than observed here). Also the slip bands are reminiscent of the strong prominent slip lines reported by Basinski, Basinski and Howie (1969) which resulted when fatigue hardened copper crystals were slightly overstrained (section 2.7). Thus it appears that the saturation structure in cyclic softened or hardened copper exists in a delicate balance and can be penetrated by any local overstress. This in turn leads to bands of localized slip from which

fatigue failure originates.

6.2 Discussion of Electron Microscopy Results

In order to examine in detail the mechanisms by which the overall macroscopic changes described above are effected, the structural evidence derived from transmission electron microscopy will be considered.

The observed dislocation substructure which developed during pre-straining is very similar to that reported by other investigators, notably Steeds (1966). The main features of the microstructure are the formation of two-dimensional "carpets" of dislocations, often separating regions of misorientation, parallel to the primary slip plane (Mic. #4) and dense walls of dislocations perpendicular to the primary plane (Mic. #5). A loose cell structure is formed parallel to the primary plane (Mic. #1) and the secondary dislocation density in the cell walls is quite high (Mic. #3). Quantitative estimates of the dislocation densities by Steeds indicate that the density of secondary dislocations is comparable to or somewhat greater than the density of primaries. Steeds concluded that the dislocation carpets were formed by the interaction between primary and secondary dislocations, with alternate walls containing forest dislocations of opposite signs. He also observed misoriented regions bounded by twist boundaries and others associated with tilt boundaries. Steeds identified the dense orthogonal walls as bands of primary edge dislocations which formed by a mutual edge trapping mechanism.

After fatigue softening at room temperature, for 1500 cycles, the microstructure observed in sections parallel to the primary plane (Mic. #6, #7) consists of a rough cell structure, similar both in scale

and in geometry to that observed after tensile deformation. The walls however, particularly along [0$\bar{1}$1], are much more densely packed and significantly, consist of a much greater density of dipoles (Compare Mic. #9, #3). The high dipole density is obvious not only within cell walls but also in the loose tangled regions and in the relatively dislocation free areas between walls (Mic. #6, #8).

Two fundamental mechanisms of dipole formation have been reported in the literature, one involving jog dragging by a screw dislocation (Gilman (1962)), the other resulting from the interaction of dislocations on parallel slip planes (Tetelman (1962)). In the former case, a moving screw dislocation can become jogged by interaction with a small loop or forest dislocation. Due to the immobility of the jog, subsequent movement of the screw dislocation causes dragging out of edge components on parallel slip planes. The resulting elongated dipole can be "pinched off" by cross-slip, leaving a dipole loop lying in the [1$\bar{2}$1] direction. Most of the loops observed are of this nature and numerous jogged screw dislocations, some in the process of loop formation, were observed in the micrographs (Mic. #12). Thus, this process accounts for at least part of the observed dipole density. The Tetelman mechanism for dipole formation involves two non-parallel dislocations gliding in parallel glide planes. If the Burgers vectors of the dislocations are equal but of opposite sign, the dislocations can lower their energy by re-orientating part of their lengths along a line bisecting the angle between the dislocations. Under certain conditions of applied stress and separation of the glide planes this arrangement will be stable. However, if segments of either dislocation near the ends of the dipole are of screw orientation, cross-slip and

the subsequent annihilation of the cross-slipped segments will produce dipole loops. Although the resulting loops can be of mixed edge and screw orientation, Tetelman concluded that the mixed dipole can lower its energy by gliding into a pure edge orientation. In view of the fact that during cycling, dislocations of opposite sign on neighbouring slip planes are continuously gliding in opposite directions and being brought into juxtaposition, much of the increased dipole density can be attributed to the Tetelman, or similar, mechanism. Evidence of just such an interaction can be seen in Micrograph #12 at point B.

In sections perpendicular to the primary plane, the structure observed in the softened state (Mic. #10) is markedly different from that seen after tensile deformation. In particular, regions of misorientation have disappeared, consistent with the decrease in asterism exhibited in the Laue spots, a clearly defined cell structure exists and cell walls are elongated primarily along the trace of the critical plane. These walls appear to consist mainly of dislocation segments aligned along the trace of the primary plane (Mic. #11) and are reminiscent of the orthogonal walls formed during tensile deformation by mutual trapping of primary edges. One possible mechanism by which a basic rearrangement of the microstructure could occur is the "sweeping up" of dislocation debris by moving dislocations, in the manner suggested by Sharp and Makin (1964). In this mechanism, Sharp and Makin show by calculation that a dipole can be trapped in the vicinity of a dislocation of the same Burgers vector, and can in fact be swept along with the dislocation if it moves. This process also explains the clear areas which separate regions of high dislocation density. Such a mechanism appears to be operative in Micrograph #12, where a large number

of screw dislocations are evident between cell walls.

The structure developed after softening at 195°K (Mic. #12) exhibit the same rough cell structure and dense dipole walls as was the case after softening at room temperature. The scale of the network has decreased, however, and the cell walls appear more dense, indicating a greater dislocation density. This is consistent with the higher observed saturation stress in the case of softening at 195°K. Feltner (1967) observed a similar result in both fatigue softened and fatigue hardened polycrystals of copper in which the saturation cell size decreased with decreasing temperature or with increasing saturation stress.

Feltner concluded, again in the case of polycrystalline copper, that the saturation microstructure which was developed by fatigue hardening or by fatigue softening at the same temperature and strain amplitude was identical. In the present case of copper single crystals, a plastic strain amplitude of $\pm$ .0025 was used, which is considered in the low amplitude range (Shinozaki (1968)). The fatigue hardened saturation state in this amplitude range, at room temperature, is characterized by patches of dislocation loops and dipoles which become more dense and more frequent as the amplitude is increased. Hancock and Grosskreutz (1969) concluded that cycling in the intermediate or high amplitude range promotes the organization of these dipole patches into a cell structure and that the change from a two-dimensional to a three-dimensional structure with increasing strain amplitude was merely one of degree. Thus, the observed structure after softening for 1500 cycles at room temperature exhibits the cell structure more characteristic of intermediate range cyclic hardening. This is not surprising, however, since the initial structure, after

tensile deformation, was cellular and the softening process at 1500 cycles may not be complete. There is evidence for such structural reversion in Micrographs #7 and #8 which show large areas of loop patches.

6.3 Correlation of Results

The basic softening process appears to be the production of, and the conversion of primary dislocations into, dipoles. This would have the effect of lowering the flow stress, since in the work hardening theory of Seeger (1963) the flow stress is mainly attributed to long range back stresses of piled up groups of primaries, while in the theory of Hirsch (Hirsch (1964), Hirsch and Mitchell (1966)), one component of the flow stress is attributed to such long range stresses (in Hirsch's theory the relative contributions of the flow stress components cannot be determined but calculations using various postulated pile-up configurations predict the possible contribution of back stresses from primaries as 20 - 50% of the flow stress). Thus, as piled up groups of primaries are converted to dipoles, the associated long range back stresses are greatly reduced and the flow stress decreases. As the back stresses are relieved, the Bauschinger effect should decrease, as observed, and misorientations across cell walls, due to an excess of dislocations of one sign, should disappear. That this does in fact happen is evident from direct electron microscopical observations, i.e. in the lack of contrast across cell walls, and from the decrease in asterism exhibited by the Laue spots. The temperature dependance of the softening rate, similar to that of τ_{III}, can also be explained on the basis of dipole formation since the likely mechanisms of dipole formation, i.e. jog-

dragging and the Tetelman mechanism, are both dependant on the cross-slip process for completion.

The large number of long dislocations, particularly screw dislocations, observed between cell walls in the fatigue softened crystals (Mic. #7, #12) indicate the strain, at least in part, at saturation is carried by dislocation motion across cell walls. This is consistent with the continued slip line action during saturation. Flip-flop motion of the dipoles or some other co-operative motion of dislocations within the cell walls may also account for part of the strain.

Evidence developed in this experiment indicates that copper single crystals fatigue soften to a saturation stress which depends only on the temperature and the strain amplitude and which is equal to the saturation stress attained by fatigue hardening under the same conditions. The microstructural observations also indicate that the structure developed during tensile deformation is at least in the process, during softening, of reverting to the structure characteristic of the saturated state in fatigue hardening. Thus the problem of structural instability and the development of coarse slip bands in the fatigue softened state is common to the situation in fatigue hardening.

6.4 The Saturated State

Unfortunately, no general agreement exists as to the detailed nature of the microstructure developed at saturation or, in particular, concerning the formation and development of persistent slip bands. Undoubtedly, some of the discrepancies can be attributed to differences in mode of testing and in stress or strain amplitude used but some

fundamental differences remain. Several of the more recent attempts to describe the saturated state will be discussed below.

Feltner (1965) devised a model to relate the mechanical behaviour directly to the observed dense dipole microstructure. In the initial rapid hardening stage, the hardening rate was determined by the rate of formation of debris obstacles, thought to be formed by some variant of the double cross-slip mechanism. As the crystal becomes filled with debris, the motion of screw dislocations diminishes and the enforced strain is accomodated by the "flip-flop" motion of the dipoles from one equilibrium position to another. The temperature dependence of the saturation stress was attributed to prismatic dislocation loop-point defect interactions but no mention was made of persistent slip band formation. Watt (1967) argues against this model on the basis of his calculations which indicate that an unreasonably high density of dipoles would be necessary to carry the enforced strain.

Avery and Backofen (1963) proposed a fatigue hardening model based on point defect production. They suppose that the internal stress is the sum of the dislocation pile-up and tangle stresses which are of "long wavelength" and a friction stress of "short wavelength" due to point defects. At low amplitudes, the dislocation mean free path is such that hardening is controlled by the short wavelength stress field. They suggest that the approach to saturation may be explained by the onset of dynamic recovery processes (cross-slip or the "sweeping up" of point defect obstacles) which eventually balance the hardening processes. Alternatively, the plastic strain may become reversible as for the case of dislocations bowing back and forth between pinning points. Basinski, Basinski and Howie (1969)

observed mottled areas of unresolved black spots in their micrographs, which they speculated were agglomerations of point defects, and concluded that many of the characteristics of fatigue hardening can be explained on this basis. Shinozaki (1968), on the other hand, felt that point defects contributed very little to the hardening process, mainly due to the fact that he observed few jogs on the strain carrying dislocations in the matrix (vacancies should diffuse to dislocations, thereby jogging the dislocation and effectively pinning the line at that point). He did observe considerable jogging of dislocations within the braids, however, and Broom and Ham (1959) reported a high density of vacancies in fatigued metals. In the present experiment the role of point defects is difficult to ascertain, simply because point defects are unresolvable in the electron microscope. A large number of jogged dislocations and small loops (jog-dragging can produce point defects or dipole loops depending on the jog height) were observed in the softened structures, however, so that point defects may well aid in the softening process and in some form of dynamic recovery mechanism at saturation. Vacancies can, for example, diffuse to a dislocation line and allow nonconservative motion of the dislocation into a lower energy configuration.

Shinozaki (1969) concluded, in the case of low amplitude fatigue of copper, that at saturation the braids which developed during hardening are no longer growing and the spacing between them is not decreasing. Strain is carried by dislocations moving back and forth between the braids or alternatively, dislocations become entangled in the braids on one half cycle while on the reverse cycle, other dislocations are pulled free from the braids to carry the strain. Raising the strain amplitude causes the

scale of the microstructure to decrease so that the braids at saturation are closer together.

Concerning the nature of the persistent slip bands which develop at saturation, basic differences of opinion exist. The main points of contention are whether the dislocation structure associated with a persistent slip band is different from that of the intervening matrix and whether the development of the persistent slip bands is a surface or a bulk phenomenon.

Laufer (1969) fatigued copper crystals in reversed bending at a load which produced a matrix structure consisting of braids elongated in the $[1\bar{2}1]$ direction. Associated with a persistent slip band (PSB) in an early stage of development was what had been called a "ladder structure", which often could be observed to blend into the matrix at a certain depth below the surface. With more developed PSB's a sandwich structure was observed, i.e. matrix-ladder-cells-ladder-matrix. The "ladders" were mainly primary edge bundles arranged in sheets parallel to $(\bar{1}01)$ or multipole walls. Laufer postulates the following sequence of events before crack formation: (1) the matrix structure develops; (2) the matrix structure becomes unstable and the braids collapse into multipole walls, which propogate into the matrix (this first step in the formation of a PSB is accompanied by surface relief, i.e. intrusions or extrusions); (3) the walls, or "ladder structure", become unstable and break up into cells enclosing volumes rotated about [111] with respect to their surroundings - the sandwich structure has now formed, and grows. Lukáš, Klesnil and Krejčí (1969) observed structures similar to that reported by Laufer in copper single crystals which they fatigued in "push-pull" in the low

stress region. They found the dislocation substructure of PSB's completely different from that in the remaining volume of the crystal, being composed of a "ladder-like" or a cell structure depending on the orientation of the foil examined. They postulate that a PSB is formed by a carpet of irregular cylinders with the axes perpendicular to the primary slip plane and that the great majority of PSB's are confined to a 200 μm thick surface layer.

Watt (1967), in his work on low amplitude fatigue of copper, determined that PSB's do not need to develop a unique microstructure different from the bulk microstructure. Rather, variations in the bulk microstructure which produce local instabilities can generate the observed differences in local strain amplitude. Also, PSB's do not necessarily form first at the surface and then grow into the interior of the specimen but may develop from centers of local high strain amplitude dispersed throughout the specimen. Watt related the saturation effect and the development of PSB's by observing that during the final stage of hardening the PSB's begin to carry an increasing share of the strain. At saturation, the hardening mechanisms continue to operate in the matrix regions but without an increase in the applied stress, since the strain which has been blocked can be produced by the developing PSB's. The only microstructural feature observed were dense clumps of dipoles.

6.5 Experimental Errors

Although the results obtained in this experiment are interpreted, by necessity, in a mainly qualitative manner, some attention should be given to the nature of the numerical errors involved. Also, since the validity of electron microscopical observations are in some doubt, as discussed more

fully in sections 2.5 and 2.6, the possible sources of error relevant to the present investigation will be discussed.

In the hardening and softening curves of figures 4.2 - 4.7, any uncertainty is due to a combination of errors in measurement of the load, measurement of the strain, calculation of the Schmid factor and measurement of the crossectional areas, and of errors due to misalignment of the specimen and to temperature fluctuations. The load could be read from the chart recorder to within $\pm$ 7 lb, giving a probable error of $\pm$ 1%, while the plastic strain amplitude could be controlled, at least during the first 100 cycles of low strain rate, to within $\pm$ 5%. This could cause an additional error in the measured load of $\pm$ 1%. An uncertainty of $\pm$ 4% in the calculation of the Schmid factor for the primary system is due mainly to errors in plotting the tensile axis by Laue back reflection techniques. Errors in the actual measurements of the crossectional areas are negligible compared to errors due to the non-uniformity of the crossection at various points along the gauge length. The crossectional area was found to vary at most by $\pm$ 5% so that an average value of five determinations is accurate to $\pm$ 3%. The specimens could be aligned in the fatigue adaptor to within an estimated .005" while the test temperature could be controlled to $\pm$ 2°K. A temperature change of this magnitude should have a negligible effect on the mechanical response of the specimen but could, at the lower temperatures (because of the different coefficients of thermal expansion of the adaptor and the specimen), cause a long range error in the softening curve of $\pm$ .5%. Neglecting errors which remain constant during a given test (errors in crossectional area, Schmid factor, alignment), and assuming an error of $\pm$ 2% in the chart recorder, the maximum error in the peak stress

for that test is ± 5%. An additional error of ± 3%, due to the crossectional areas, is introduced when comparing the saturation stresses at the various temperatures.

Apart from the purely mechanical errors involved in electron microscopy, such as chromatic aberration, spherical aberration and astigmatism (Hirsch, Howie, Nicholson, Pashley and Whelan (1965)), of particular concern to the present work is the loss and rearrangement of dislocations during thinning and the assumption that observed dislocation structures are representative of the bulk sample. In the present case, the observed dislocation distributions are well developed structures, on a scale small with respect to the area of the foils. Thus, rearrangement should be slight and the important characteristics of the microstructure should remain intact during thinning. The thin foils which were examined were prepared from sections cut at random from near the center of the specimen gauge lengths and care was taken to examine as large areas and as many areas as possible. While it is necessary to make the assumption that the dislocation microstructure is homogeneous on a scale comparable to the foil dimensions (which is reasonable in view of the uniform fine slip activity at the stage of cycling considered), it is felt that the dislocation distributions and the Burgers vector determinations shown are representative of the crystal as a whole.

6.6 Summary

It was the philosophy of the present research to derive as much information as possible concerning the mechanisms of fatigue softening and the fatigue softened state from a simple system. Copper single crystals

were prestrained in uniaxial tension and softened by low amplitude "push-pull" fatigue. The mechanical response of the specimens as a function of temperature was correlated with X-ray and slip line results and quantitative electron microscopy was employed to determine details of the microstructural changes which occur during softening. A self consistent explanation, based on the microscopical observations, was proposed to account for the fatigue softening behaviour of copper single crystals.

A main contribution of this thesis is the identification of dipole formation as the major softening mechanism occuring in copper. Cross-slip, as a necessary process in most methods of dipole formation, is believed to account for the temperature dependence of the softening rate. This suggests that any factors which make cross-slip more difficult (i.e. decreased stacking fault energy) should cause a corresponding decrease in softening rate. Equally important, particularly from an engineering standpoint, is the result that during softening, the dislocation structure reverts to that characteristic of the fatigue hardened state. Thus, the problem of structural instability leading to development of persistent slip bands and ultimate failure, is common to both situations.

CHAPTER 7

CONCLUSIONS

1. Copper single crystals, prestrained in tension to 4.5 kg/mm^2, soften when fatigued at constant plastic strain amplitude of $\pm$ .0025.

2. The softening rate decreases and the saturation shear stress increases as the temperature decreases. At a given temperature and strain amplitude, the saturation stress is the same for fatigue hardening and fatigue softening.

3. Softening is effected by the creation of, and conversion of primary dislocations into, dipoles which are formed by a cross-slip process. Long range back stresses due to primary pile-ups are thus relieved, resulting in a decrease in flow stress and the disappearance of the Bauschinger effect.

4. At 1500 cycles, the softened microstructure is characterized by dense walls of dipoles arranged in a rough cell structure and some regions of broad dipole mats. The cell walls in (111) sections are aligned predominantly along $[0\bar{1}1]$ and $[\bar{1}10]$ directions. The dislocation distribution is thus in the process of reverting to the structure typical of the saturation state in low amplitude fatigue hardening.

5. Coarse slip bands, similar to persistent slip bands which form during fatigue hardening, are evident at 4500 cycles.

CHAPTER 8

PROPOSALS FOR FUTURE WORK

1. In strongly neutron irradiated crystals, moving dislocations remove defects (point defects, small loops) which were produced by the neutron bombardment and leave cleared traces that are visible in the electron microscope (Seeger (1963)). By irradiating a fatigue softened copper crystal and straining for an additional cycle, it should be possible to determine, by electron microscopy, if the strain carrying elements at saturation are dislocations moving between cell walls (or braids). This technique could be used also to check the hypothesis that an overstress will "upset" the structural balance established during uniform cycling, allowing strain in effect to penetrate the dense dipole walls. (These experiments were attempted in conjunction with the present research but a suitable " defect background" could not be achieved in the crystals tested, with the neutron flux available in the McMaster University reactor).

2. Extending the present experiment over a wider range of temperatures and analysing the resulting kinetics in some detail should provide useful information concerning the relative contributions of cross-slip, climb and point defects to the softening process.

3. Detailed electron microscopical investigations should be carried

out to determine if fatigue softened and fatigue hardened copper crystals develop persistent slip bands by identical processes. Such an investigation would establish the similarity between the hardened and softened states at saturation, as well as providing valuable information on the mechanisms of fatigue failure.

BIBLIOGRAPHY

Avery, D. H. and Backofen, W. A., 1963, Acta Met., 11, 653.

Basinski, S. J., Basinski, Z. S. and Howie, A., 1969, Phil. Mag., 19, 899.

Basinski, Z. S., 1964, Discussions of the Faraday Society, Dislocations in Solids #38, 93.

Basinski, Z. S., 1965, Seminar of the American Society for Metals, Recrystallization, Grain Growth and Textures,

Broom, T. and Ham, R. K., 1959, Proc. Roy. Soc., A251, 186.

Broom, T. and Ham, R. K., 1962, Phil. Mag., 7, 95.

Bullough, R. and Sharp, J. V., 1965, Phil. Mag., 11, 605.

Byrne, J. G., 1965, Recovery, Recrystallization and Grain Growth (Macmillan), 37.

Clarebrough, L. M. and Hargreaves, M. E., 1959, Prog. Met. Phys. 8, 1.

Feltner, C. E., 1965, Phil. Mag., 12, 1229.

Feltner, C. E. and Laird, C., 1967, Acta Met., 15, 1621.

Gilman, J. J., 1962, J. Appl. Phys., 33, 2703.

Ham, R. K., 1966, Can. Met. Quart., 5, 161.

Hancock, J. R. and Grosskreutz, J. C., 1969, Acta Met., 17, 77.

Hirsch, P. B., 1963, N.P.L. #15, The Relation Between the Structure and Mechanical Properties of Metals, 39.

Hirsch, P. B., 1964, Discussions of the Faraday Society, 38, 111.

Hirsch, P. B., Howie, A., Nicholson, R. B., Pashley, D. W. and Whelan, M. J., 1965, Electron Microscopy of Thin Crystals (Butterworth).

Hirsch, P. B. and Mitchell, T. E., 1966, Metallurgical Society Conference, Work Hardening (Gordon and Breach), 46, 65.

Johnston, W. G. and Gilman, J., 1960, J. Appl. Phys., 31, 632.

Laufer, E., 1969, Czech. J. Phys., 19, 333.

Lukáš, P., Klesnil, M. and Krejčí, J., 1969, Czech. J. Phys., 19, 335.

Mader, S., Seeger, A. and Leitz, C., 1963, N.P.L. #15, The Relation Between the Structure and Mechanical Properties of Metals, 3.

Metallurgical Society Conference, 1966, Work Hardening (Gordon and Breach), 46, 1.

Mitchell, T. E. and Thornton, P. R., 1963, Phil. Mag., 8, 1127.

Mughrabi, H., 1968, Phil. Mag., 18, 1211.

Nabarro, F. R. N., Basinski, Z. S. and Holt, D. B., 1964, Advances in Physics, 13, 193.

Seeger, A., 1963, N.P.L. #15, The Relation Between the Structure and the Mechanical Properties of Metals, 3.

Sharp, J. V. and Makin, M. K., 1964, Phil. Mag., 10, 1011.

Shinozaki, D., 1968, M.Sc. Thesis, McMaster University, Hamilton, Canada.

Shinozaki, D. and Embury, J. D., 1969, Metal Science Journal, 3, 147.

Snowden, K. U., 1963, Acta Met., 11, 675.

Steeds, J. W., 1966, Proc. Roy. Soc., A292, 343.

Steeds, J. W. and Hazzledine, P. M., 1964, Discussions of the Faraday Society, Dislocations in Solids #38, 103.

Tetelman, A. S., 1962, Acta Met., 10, 813.

Watt, D. F., 1967, Ph.D. Thesis, McMaster University, Hamilton, Canada.

Watt, D. F., Embury, J. D. and Ham, R. K., 1968, Phil. Mag., 17, 199.